UNIVERSITY OF GOTHENBURG

DEPARTMENT OF BIOLOGICAL AND ENVIRONMENTAL SCIENCES

DOES MUSSEL FARMING INFLUENCE CARBON DIOXIDE, METHANE AND NITROUS OXIDE INVENTORIES?

A case study on the Swedish west coast.

Nick Rainer Törpel

Degree project for Master of Science (120 hec) with a major in Environmental Science

ES2510 Examination course in Environmental Science (60 hec)

Second cycle

Semester/year: Autumn 2023

Supervisor: Stefano Bonaglia

Examiner: Lennart Bornmalm

AI-generated image, created by Copilot | Designer with the following prompt: “a watercolor painting of a single blue mussel in the ocean”, available at: https://www.bing.com/images/create.

Abstract

Both climate change, caused by anthropogenic emissions of greenhouse gases (GHGs), and food security remain substantial challenges for the global community. Against this backdrop, aquaculture is seen to present some remedies. Of particular interest is the farming of marine bivalves, such as blue mussel (Mytilus edulis), since they can be a source of nutrition and have the potential to provide other ecosystem services. However, the effect of blue mussel farming on GHG emissions is not widely studied. This study aims to investigate if mussel farming directly leads to higher emissions of the three major GHGs, carbon dioxide (CO_2), methane (CH_4), and nitrous oxide (N_2O). Concentrations of these gases were measured around two active and commercially used mussel farms on the Swedish west coast that produce blue mussels for human consumption, to investigate if mussel farming influences greenhouse gas dynamics. A control site, not impacted by aquaculture, was chosen for each of the mussel farms. For data collection and sampling three different measuring campaigns were undertaken in September 2023, October 2023 and in February 2024 to account for variations in temperature, water column conditions, and the status of the mussel farms. Discrete water samples were collected from a research vessel at each studied area, at three different depths for later analysis of dissolved inorganic carbon (DIC), dissolved CH_4 and N_2O in the water column via single-phase gas chromatography and solid-state infrared detection. Additionally, in situ measurements of the surface water concentrations for the three GHGs were conducted at both farms and both control areas using optical feedback-cavity enhanced absorption spectroscopy (OF-CEAS). The mussel farms were found to not have an environmentally significant impact on the local marine GHG dynamics, suggesting that the aquaculture of bivalves, and blue mussels in particular, can be a sustainable source of protein.

Popular science summary

Save the climate, eat more mussels!

Climate change is a hot topic today, both literally and figuratively, as it can lead to an increase in global temperatures, which in turn can lead to many difficult challenges for humanity. The main cause of climate change is the increased emission of greenhouse gases, which can trap heat within earth's atmosphere, just like the roof and the walls of the greenhouse in your garden trap heat. The three most important and impactful of these greenhouse gases are carbon dioxide, methane, and nitrous oxide.

These greenhouse gases are not only emitted from the exhaust pipe of your car or from dirty coal power plants. The production of food can also contribute to these emissions, especially methane. Some foods are associated with higher emissions than others, and the production of protein sources, like meat and fish, is known to emit more than the production of plant-based food. Aquaculture, the farming of animals that live in the water, on the other hand, has not been studied as much, and there is still a lot we do not know when it comes to the greenhouse gas emissions from this sector. Even though most forms of aquaculture focus on different species of finned fish, like salmon or trout, the farming of bivalves, shellfish like mussels, clams, or oysters, is an industry that is on the rise and has great potential to produce high quality protein with lower climate impact. One of the most common species of bivalves, farmed in northern Europe and North America, is the blue mussel. If you have ever had the famous Belgian dish Moules-frites, you should be familiar with this mussel. It is grown on long ropes suspended in the water by buoys and anchored to the seafloor. Such "mussel farms" can also be found in the fjords at the Swedish west coast, like the Koljöfjord in this study.

Here I investigated the potential contribution of mussel farming to greenhouse gas emissions at two commercial mussel farms. For this investigation, I collected water samples at different depths at the mussel farms and at two reference areas. Reference areas were not impacted by aquaculture and represented the natural conditions in the fjord. This was done from aboard "R/V Alice", a boat equipped with tools and instruments for scientific research, which belongs to the University of Gothenburg.

The collected samples were later analyzed in the laboratory at the University of Gothenburg to determine the amount of the different greenhouse gases dissolved in the water. The measured concentrations of carbon dioxide, methane, and nitrous oxide in the water at the two mussel farms were compared with the reference areas. I expected the concentrations of the three major greenhouse gases to be higher at the mussel farms than at the reference areas, but surprisingly, no meaningful difference was found. This would suggest that mussel farming does not lead to higher emissions of greenhouse gases and does not affect the climate in a negative way.

So, the next time you order Moules-frites on your summer vacation to Belgium or your weekend trip to the coast, you can rest easy knowing that you chose one of the most environmentally friendly sources of protein.

Table of Contents

1. Introduction and Aims 1
2. Materials and Methods 4
   2.1. Site description 4
   2.2. Measuring campaigns 5
   2.3. Cruises, research vessel & equipment 6
   2.4. Sampling, measuring & data collection 6
      2.4.1. Discrete water samples 6
      2.4.2. Conductivity, Temperature, Depth (CTD) 7
      2.4.3. Continuous in situ measuring 7
      2.4.4. Spatial data (GPS) 8
   2.5. Data analysis & statistics 8
      2.5.1. Dissolved Inorganic Carbon (DIC) 8
      2.5.2. Gas Chromatography (GC) 8
      2.5.3. Maps and plots 9
      2.5.4. Statistics and data analysis 9
3. Results 10
   3.1. Continuous in situ measurements 10
      3.1.1. Carbon dioxide (CO_2) 10
      3.1.2. Methane (CH_4) 12
      3.1.3. Nitrous oxide (N_2O) 14
   3.2. Discrete samples 16
      3.2.1. CTD-data (oxygen, salinity, and temperature) 16
      3.2.2. Dissolved inorganic carbon (DIC) 18
      3.2.3. Methane (CH_4) 20
      3.2.4. Nitrous oxide (N_2O) 22
4. Discussion 24
   4.1. Carbon dioxide and dissolved inorganic carbon (CO_2 & DIC) 24
   4.2. Methane (CH_4) 25
   4.3. Nitrous oxide (N_2O) 27

5. Opportunities and Limitations 28
6. Conclusion 29
7. Acknowledgments 29
8. Reference list 30

1. Introduction and Aims

The increasing anthropogenic emissions of greenhouse gases (GHGs) into the atmosphere are recognized as the main contributor to ongoing global climate change (Hoegh-Guldberg and Bruno, 2010). These gases trap heat in the Earth's atmosphere and contribute to the rising global temperatures. The three major GHGs, namely carbon dioxide (CO_2), methane (CH_4), and nitrous oxide (N_2O), are of particular concern due to their potency and widespread occurrence (EPA, 2023). The increase in atmospheric CO_2 since pre industrial times is mostly due to anthropogenic activities such as burning fossil fuels and land use change (Intergovernmental Panel On Climate Change, 2022). Primary sources of anthropogenically produced CH_4 and N_2O are agricultural practices, including livestock farming, and the use of synthetic fertilizer (Malyan et al., 2016; Smith, 2005). As animal protein plays a crucial role in human nutrition on a global scale (Babinszky et al., 2011), and it provides essential nutrients such as amino acids, vitamins, and minerals, which are difficult to obtain through a plant-based diet (Wood, 2017), it will continue to be a driver for GHG emissions (Gerber et al., 2013; Zhuang et al., 2017).

The global demand for seafood has doubled since the year 2000, and is expected to double again by 2050 (Naylor et al., 2021). More than 15 percent of the world's total animal protein consumption comes from seafood (Béné et al., 2016); however, the annual amount from capture fishery has flattened since the late 1980s and has been hovering right below 100 megatons (Mt) per year for the last four decades (FAO, 2022). This is likely due to the fact that half of all commercial marine species could be considered to be over-fished (Srinivasan et al., 2010), as approximately 80 % of the global fisheries are not able to withstand an increase in fishing activities and only around 17 % of the world’s fisheries can support any sort of growth in production (Freitas et al., 2008). In contrast, the annual production from aquaculture, the husbandry and farming of aquatic animals and plants, has increased steadily over the past years and is now on par with capture fishery. When including algae, aquaculture even surpasses capture fishery, with a total production of 122.6 Mt live weight equivalent (weight, when removed from water) in 2020. The largest portion of this total production was the farming of finfish (57.5 Mt; 47%), followed by algae (35.1 Mt; 29%), mollusks (17.7 Mt; 14%) and crustaceans and other animals (12.3 Mt; 10%) (FAO, 2022). Between 1990 and 2009 aquaculture was the fastest growing livestock sector in the world (Little et al., 2016).

Although the majority of aquaculture focuses on different species of fish and algae, the farming of mussels still resulted in 1.5 Mt of live weight equivalent for the year 2020 (FAO, 2022). Many consider mussel farming to be more sustainable than traditional aquaculture that focuses on fish, since mussels are filter feeders, which eliminates the need for external input of feed (Lindahl et al., 2005). An additional benefit of mussel farming is the ability to mitigate eutrophication (Fennel and Testa, 2019). Overall, the mussel farming sector has seen an increase in volume by four times over the past four decades (Suplicy, 2020), covering both freshwater and marine environments.

Globally, different species of mussels are farmed, with the blue mussel (*Mytilus edulis*) being the most common species in northern Europe (FAO, 2024). While there is research concerning the impact that mussel farming can have on sediment biogeochemistry and the benthic

environment (Hylén et al., 2021), there seems to be a lack of knowledge when it comes to the potential GHG emissions from mussel farms (Ray et al., 2019).

Different studies have compared the associated GHG emissions from bivalve aquaculture with those arising from terrestrial livestock protein production. For example, Ray et al. 2019 compared their findings on the emissions from oyster farms with the emissions connected to poultry, pork, mutton, and beef production, described by Opio et al., 2013, and MacLeod et al. 2013, and found that oyster had by far the lowest emission per kg of produced protein. In another study, Yaghubi et al., 2021 compared the GHG emissions per kg of edible product of blue mussels, tofu, eggs, salmon, poultry, pork, lamb, and beef based on data from four other sources (Fry, 2012; Gorissen and Witard, 2018; Mejia et al., 2018; Suplicy, 2020). They concluded that only tofu production leads to lower emissions of GHGs than blue mussel farming.

In general, the natural habitat of the blue mussel includes areas allowing for the attachment to hard substrates such as rocks, piers, and other stable surfaces in the ocean or estuaries. It prefers cooler water temperatures and can often be found in densely packed beds, which provide protection and stability for the community. In the context of mussel farming, structures such as ropes, poles or nets are used to create artificial habitats for the mussel banks (FAO, 2024). Blue mussel larvae attach or are attached to these structures and grow until they are large enough to be harvested, which usually occurs when the mussels reach maturity at around 12 to 15 months (FAO, 2024) or later.

Marine mussel farming is bound to coastal regions due to the mussels' natural habitat and the need for accessibility of the farms from land. Since marine mussel farms in general are bound to the coastal regions, it is important to discuss the role of GHGs within the coastal environment. This master thesis thus focuses on the role of mussel farming in shaping GHG dynamics at two Swedish coastal sites. The coastal ocean plays a significant role in the global carbon cycle, including the absorption, release, and storage of carbon dioxide (CO_2) (Borges et al., 2005), and acts as an interface between the terrestrial environment and the open sea. The exchange of CO_2 between the air and the ocean is impacted by factors such as temperature, salinity, and biological activity. Ocean acidification is another important aspect of the interplay between CO_2 and the sea. It is the uptake of anthropogenic CO_2 by the ocean, which leads to a lowering of the pH, making the ocean more acidic (Doney et al., 2009; Dore et al., 2009). This can have serious effects on marine ecosystems, particularly organisms that rely on calcium carbonate structures, such as the blue mussel itself (Hofmann and Schellnhuber, 2009; Kroeker et al., 2010). The coastal ocean is subject to a complex interplay of biogeochemical processes that determine its role in the global carbon cycle and how it is affected by increasing levels of atmospheric CO_2.

Methane is also present in considerable amounts in the coastal ocean and can have both natural and anthropogenic sources. Natural sources include methanogenesis in anoxic sediments, where microorganisms produce methane during the decomposition of organic material (Hovland et al., 1993). Anthropogenic sources can include runoff containing organic waste, for instance

from terrestrial farming, or discharges from industrial activities (Shahidul Islam and Tanaka, 2004); however, methane released into the water column does not always reach the atmosphere because it can be oxidized by bacteria that are present in the water or in sediments. This biological methane oxidation acts as a filter, reducing the amount of methane that escapes into the atmosphere (Mao et al., 2022). On one hand, mussels may enhance methane oxidation as they lay in the oxic water column, and they may act as substrate for CH_4 oxidizers. Some information on the GHG emissions from other types of bivalve farming exists. For example, it was found that oysters in aquaculture do not emit any CH_4 (Ray et al., 2019). On the other hand, it has been shown that bivalves such as clams may emit methane because of their bacterial symbiont activity (Bonaglia et al., 2017). It is therefore especially important to investigate in which way mussel farming contributes to these emissions, so that strategies to mitigate CH_4 emissions from coastal zones can be developed.

Coastal waters can be a significant source of nitrous oxide (N_2O). The release of this greenhouse gas is influenced by various factors, including nitrate and ammonium concentrations and oxygen levels. The main drivers for the emissions are the processes of nitrification, where ammonia is converted to nitrate by bacteria, and denitrification, where nitrate is reduced to nitrogen gases. (Bonin et al., 2002). Coastal eutrophication, the over-enrichment of waters with nutrients (such as nitrogen and phosphorus), can lead to conditions that favor these processes, and coastal regions can thus be hotspots for N_2O emissions due to the high levels of nutrients that can enter the coastal zone from rivers, wastewater discharges, atmospheric deposition, and aquaculture (Murray et al., 2015). So far only one study investigated the role of blue mussels on N_2O dynamics in the coastal ocean (Voet et al., 2023). However, the findings suggest that mussel-related N_2O emissions can have a major impact on local GHG dynamics. This could be especially important in the context of a potential future increase in global mussel farming and should be investigated further.

The aim of this study is to determine if mussel farming directly leads to higher emissions of the three major GHGs - CO_2, CH_4 and N_2O. In order to do this, the concentrations of the studied gases were analyzed in the water column by means of single-phase gas chromatography and solid-state infrared detection. Additionally, the surface water around two active mussel farms on the Swedish west coast were analyzed by means of optical feedback-cavity enhanced absorption spectroscopy (OF-CEAS) and compared to the non-impacted control sites. I hypothesized that the concentrations of GHGs in the waters, that are directly influenced by the mussel farms, would be higher compared to the concentrations at the non-impacted control areas and intended to investigate whether this hypothesis can be confirmed.

2. Materials and Methods

2.1. Site description

Field work was conducted on the Swedish west coast, and Kristineberg Center for Marine Research (58°14'58.96"N, 11°26'44.18"E) in the small village of Fiskebäcksil served as the base for all three expeditions. The center is in proximity to two mussel farms. Both farms are used commercially to grow blue mussels for human consumption and are operated by *Scanfjord*, a local company. The two farms will be referred to as Farm A and Farm B throughout this report. Farm A is situated in the Koljöfjord (58°13'31.37"N, 11°32'38.52"E) and Farm B is in the Borgilefjord (58°15'38.17"N, 11°37'52.69"E). Both the Koljö- and the Borgilefjord belong to the Orust fjord system (Hansson et al., 2013). A non-impacted control area was chosen for each farm. These reference areas will be referred to as Control A (58°13'33.03"N, 11°33'2.77"E), and Control B (58°15'31.12"N, 11°38'20.11"E). Farm and control areas have comparable depths of around 10 m. The following abbreviations will be used for Farm A, Control A, Farm B and Control B throughout this text: AF, AC, BF and BC.

The four sampling areas were chosen according to a number of criteria: both mussel farms were known to be in active use at the time of the study, and they were in relatively close proximity to Kristineberg Center. This made it feasible to visit the farms by boat, perform the sampling and return to the center within one workday. The locations of the two mussel farms were also deemed to be very representative of the Swedish west coast while still not being too far apart.

Ideally, control areas should be situated upstream from the impacted farm areas, to completely avoid the possibility of any influence from the farm areas on the controls. However, since the studied areas are in a marine system, that is subject to some mixing of the water column from tidal activity and weather events (Hansson et al., 2013), no true upstream location for the controls can be achieved. Thus, the control areas were chosen to be about 250 - 300 away from the farms. At the same time, they needed to be relatively close to the farms, so that they would have comparable depths to their respective impacted areas.

The individual mussel farms are built according to the “Scanfjord system”, a type of longline mussel farming system that was first developed in the 1970s in Sweden. A mussel farm of this type normally consists of ten long parallel support lines that are kept afloat horizontally in the water column with buoys and secured to the sea floor with plough anchors. Smaller lines, on which the mussels grow, are suspended vertically from the support lines (Scanfjord, 2024). While farm A consists of only one such long line set up, farm B consists of two, so 20 long lines in total, however, the two farms support a comparable amount of mussels, since not all lines are being used. In September 2023 the mussels in the two studied farms were around 29 months old and the total biomass per farm was approximately 150 tons (A. Granhed, personal communication, October 27, 2023). Harvesting of the mussels took place between the second and third campaign (A. Granhed, personal communication, February 12, 2024). Other anthropogenic activities in the area include small scale maritime traffic, like leisure boating and public ferries, and terrestrial agriculture and livestock farming.

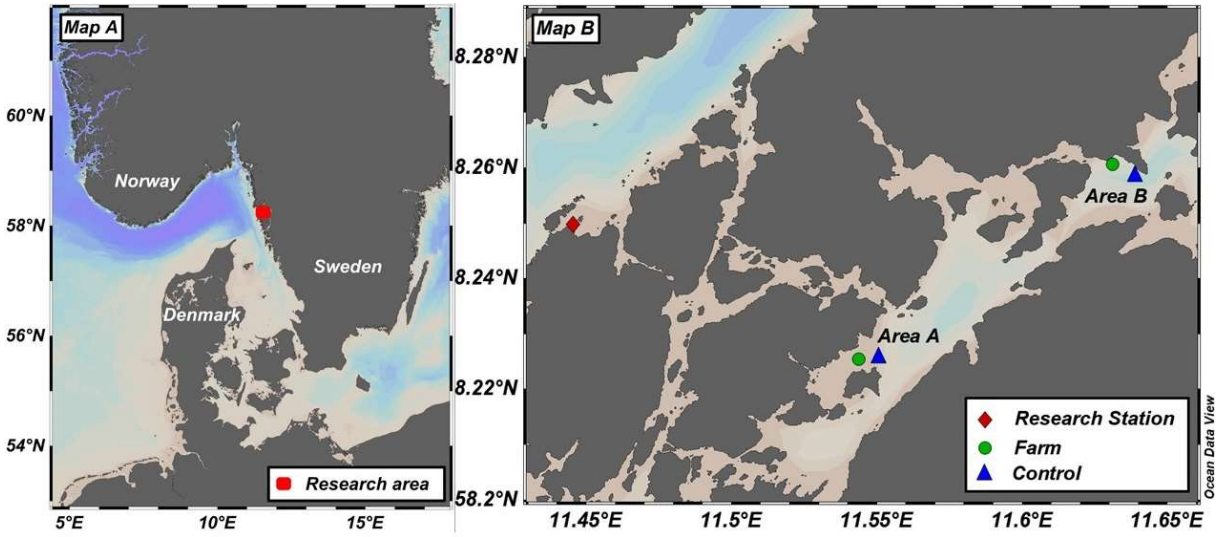

Figure 1 Maps representing the position of the research area on the Swedish west coast in relation to Norway and Denmark (Map A), and a more detailed overview of the research area (Map B).

2.2. Measuring campaigns

To account for seasonal variations in weather and temperature, as well as the production cycle in the mussel farms, three different measuring campaigns were conducted. An overview of the measuring campaigns is shown in Table 1.

Table 1 Three different measuring campaigns according to seasons, dates, corresponding status of the mussel farms, and water column conditions.

Campaign Number	Season	Time	Farm status	Water column conditions
1	Late summer	7th September 2023	Pre harvest	Stratified
2	Autumn	25th & 31st October 2023	Pre harvest	Mixed
3	Winter	14th & 15th February 2024	Post harvest	Mixed

In campaign one (September 2023) the mussels were around 29 months old (A. Granhed, personal communication, October 27, 2023). At the same time, the sea water was stratified due to the calmer weather conditions, suggesting that we would expect higher contribution of mussel respiration to the gathered data due to the accumulation of the gas within the sea water layers. In campaign two, the mussels were at a similar age as in campaign one, but the sea water was more mixed, due to harsher weather conditions, suggesting the detected impact of mussels on greenhouse gas emissions would be lower due to constant mixing of the seawater. In campaign three, most of the mussels had been harvested (A. Granhed, personal communication, February 12, 2024), therefore the impact of the remaining mussels on the greenhouse gas emissions would be minimal. Additionally, the seawater in campaign three was still relatively mixed, suggesting less accumulation of the gases between the seawater layers. Overall, I expected that the contribution of mussel farming to greenhouse gas emissions would be clearly visible in the surface water.

The in-situ measurements gave us an overview of the gas distribution on a larger scale in the farms and control sites, while the discrete samples result in a more focused view of the concentrations.

2.3. Cruises, research vessel & equipment

The main part of each measuring campaign consisted of expeditions from Kristineberg Center to the mussel farms and the control sites. These cruises were performed with the research vessel Alice. The boat had a length of twelve meters and was equipped for physical, chemical, and biological sampling. The boat's equipment included a hydraulic winch and a moveable A-frame for deck lifting, as well as a CTD (Sea-Bird 19 plus V2 200 kHz) and a rosette water sampler (SBE 55, 6 bottles). R/V Alice is owned by the University of Gothenburg and stationed at Kristineberg Center (University of Gothenburg, 2023).

2.4. Sampling, measuring & data collection

2.4.1. Discrete water samples

Discrete water samples for the analysis of dissolved inorganic carbon (DIC), methane (CH_4) and nitrous oxide (N_2O) were taken in triplicates at three different depths at each farm and each control site. The schematic drawing of the sampling at the site is shown in Figure 2. The three depths are referred to as surface, middle and bottom. Surface water was taken at a depth of two meters, the middle water was taken at five meters deep, and the bottom water was collected from a depth of approximately ten meters. This work was performed with the help of the rosette water sampler. The last of the three compounds that this study aims to investigate is CO_2. However, we do not have the ability to analyze the concentration of CO_2 in the discrete samples, like we can with the concentration of CH_4 and N_2O. Instead, we analyze the concentration of dissolved inorganic carbon (DIC). DIC is the total amount of CO_2, bicarbonate (HCO^{3-}), and carbonate (CO_3^{2-}) that is dissolved in the sea water (Carlson et al., 2001). As such, for the sake of this study, a higher concentration of DIC at a certain site or depth could point to a higher concentration of CO_2.

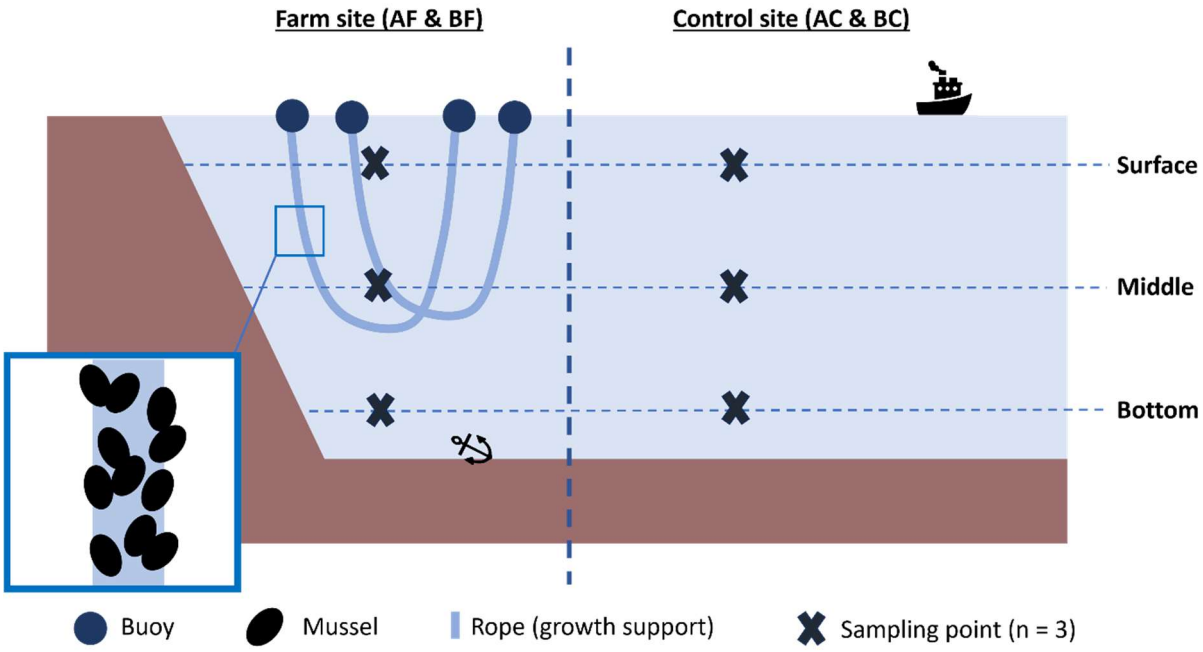

Figure 2 Schematic drawing of a mussel farm and a control site, showing the three different depths where discrete water samples were taken.

Water samples for DIC analysis were collected in 12 ml exetainers and stored at 5˚C. Samples for the CH_4 and N_2O concentrations were collected into 22 ml glass vials, fixed with 0.2 ml of zinc chloride ($ZnCl_2$) and stored at 5˚C.

2.4.2. Conductivity, Temperature, Depth (CTD)

Using the Sea-Bird 19 plus V2, we collected CTD data such as salinity, temperature, depth, and oxygen concentration, these data are relevant in its own way to explain dynamics of GHGs and is also needed for data calculation and conversion of the greenhouse gas concentrations.

2.4.3. Continuous in situ measuring

While taking the discrete water samples around the mussel farms and the control site, continuous in situ measuring of the greenhouse gas concentrations in the surface water was performed using a couple of LI-COR portable trace gas analyzers (LI-COR Biosciences). A LI-COR model LI-7810 was used for the measuring of CO_2 and CH_4, and a model LI-7820 for N_2O. The measurements were performed with one-minute intervals. In a closed loop according to (Santos et al., 2012). The seawater was pumped up from a depth of about 0.7 - 0.8 m, with a submersible pump at a rate of about 5 - 6 m^3/h. This water flowed into a water spray chamber (Durridge, RAD AQUA exchanger), there the chamber's nozzle or "shower head" aspirates the water into droplets to maximize gas equilibration. Since the instruments were placed on deck of the research vessel the temperature inside the spray chamber was found to be the same as the in-situ water temperature. Subsequently the gas was pumped from inside the spray chamber to a desiccant unit (Drierite) to remove moisture, and then further to the two trace gas analysers. A Durridge RAD7 radon detector was also used in this loop, but only to act as a pump to help transport the gases from the spray chamber to the trace gas analysers. No data was collected form the RAD7. Figure 3 shows a schematic plan of this closed loop system.

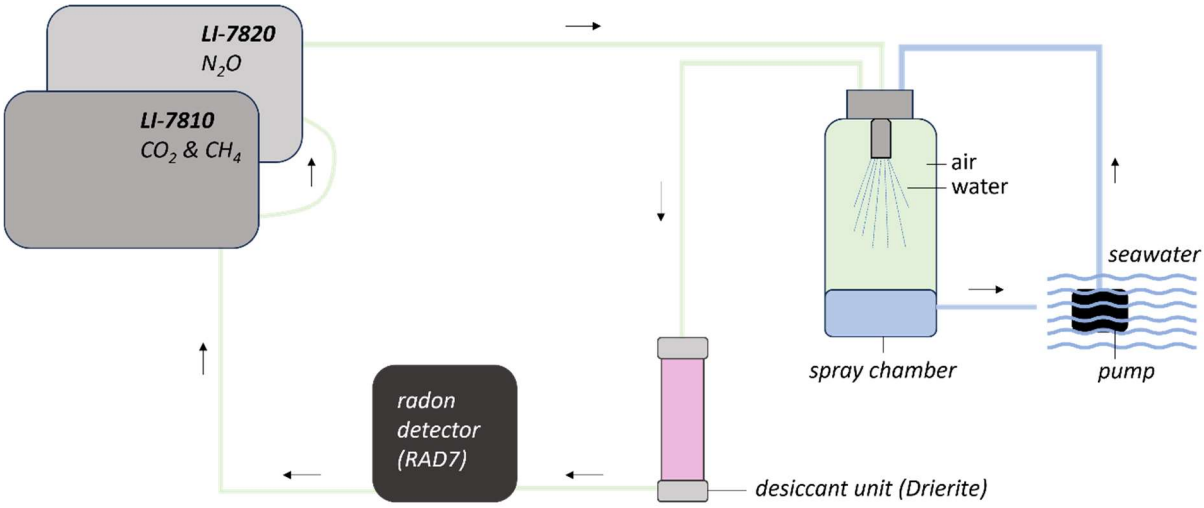

Figure 3 Schematic drawing of the closed loop measuring system for the in situ measuring of CO_2, CH_4, and N_2O in the surface water. The measuring process starts with seawater being pumped into the spray chamber, where gas equilibration takes place. The gas is pumped into the desiccant unit to remove moisture, while the water exits the chamber and runs back into the sea. The RAD7 is only used for its internal pump that helps to transport the gas through the loop, and it provides no data. Lastly the gas enters the twin linked LI-COR analyzers where surface GHG concentrations are being measured and stored.

The LI-COR trace gas analyzers use optical feedback-cavity enhanced absorption spectroscopy (OF-CEAS) to produce high-precision measurements of the partial pressure of CH_4 and N_2O in parts per billion (ppb) and CO_2 in parts per million (ppm). Conversion from partial pressure to dissolved concentration in nanomoles per liter (nM) for CH_4 were conducted using the solubility coefficients according to (Yamamoto et al., 1976). For the conversion to N_2O concentrations in nM I used the solubility coefficient according to (Weiss and Price, 1980). The concentration of CO_2 in micro atmospheres (µatm) was calculated according to (Weiss, 1974).

2.4.4. Spatial data (GPS)

To align the data from the LI-COR analyzers with positional data, a handheld Garmin GPS unit was used. Data and GPS data were later aligned with one another based on time.

2.5. Data analysis & statistics

2.5.1. Dissolved Inorganic Carbon (DIC)

The concentrations of DIC from the discrete water sampling were analyzed by a Total Dissolved Inorganic Carbon Analyzer (Appollo AS-C5) in the marine science lab of the University of Gothenburg. As the standard for this analysis, certified reference material (CRM) from Dickson Laboratory, Scripps Institute of Oceanography was used. The analytical precision was set to 0,005 %. The Apollo AS-C5 generates datasheets containing the DIC concentration for each sample µM.

2.5.2. Gas Chromatography (GC)

A headspace technique was used for the single-phase gas chromatography analysis of CH_4 and N_2O in the water column. Here 5 ml of water was withdrawn from every 22 ml glass vial with a syringe and a 0.8 x 40 mm needle through the rubber septum in the cap of the vial.

Simultaneously pure N_2 gas was injected through the septum and into the vial via an additional needle of the same size. The vials were shaken and then left overnight to ensure equilibration. This resulted in a gaseous headspace of 5 ml in every vial from which a headspace portion was injected into a gas chromatograph (Thermo Scientific Trace1300) via a robotic autosampler (Thermo Scientific TriPlus RSH). The gas chromatograph (GC) was equipped with a flame ionization detector (FID). For calibration of each measurement run, gas standards of 1.9 ppm and 50.0 ppm of CH_4 and 0.3 ppm and 4.7 ppm of N_2O were used (Air Liquide Gas AB). The Trace1300 produces partial pressure results for the studied gases in ppm. The molar N_2O concentrations for the original sample (C_{N_2O}) were calculated after (Walter et al., 2006):

$$C_{N_2O} = \frac{\beta \cdot x \cdot P \cdot V_w + \frac{xP}{RT} \cdot V_h}{V_w}$$

Concentrations in nM of dissolved CH_4 in the water ($CH_{4\ w}$) were calculated from the mole fraction of CH_4 in the headspace ($CH_{4\ h}$) and from the molar volume of methane (24.04 L/mol) at 1 atm and 20 °C:

$$CH_{4\,w} = \frac{CH_{4\,h} \times V_h}{V_w \times 24.04}$$

The variables for the calculation of the molar concentrations can be found in Table 2.

Table 2 Explanation of the variables used to calculate molar concentrations for CH_4 and N_2O samples analyzed via single-phase gas chromatography.

Variable	**Explanation**
β	Bunsen solubility in nM/atm (Weiss and Price, 1980)
x	Dry gas mole fraction of N_2O in the headspace in ppb
P	Atmospheric pressure in atm
R	Gas constant of 8.205 x 10^{-2} L atm mol^{-1} K^{-1}
T	Temperature during measurement
V_w	Volume of water in the vial
V_h	Volume of the headspace in the vial

2.5.3. Maps and plots

All maps were created with *Ocean Data View* (ODV) version 5.6.7. Statistical analysis was performed using *SigmaPlot* version 15.0 and plots for CTD-data and discrete sampling were also created with this software. Microsoft Excel was used to create a regression plot.

2.5.4. Statistics and data analysis

Two different types of statistical test were performed to determine if there are significant differences between the farm sites and the controls. The data sets from the discrete water sampling were analyzed with Welch's t-test, since they passed a Shapiro-Wilk test and thus show a normal distribution, but equal variance is not assumed. Mann-Whitney Rank Sum tests

were used for the data sets from in situ measurements, since they are not normally distributed as they all failed a Shapiro-Wilk test. To determine if statistical significance is present between two data sets, a P-value of 0.05 was chosen. If the P-value is less than 0.05, the difference is deemed to be statistically significant.

3. Results

This section consists of two main parts. The first part focuses on the results of the continuous in situ measurements, while the second part focuses on the results from the discrete sampling. Within each part the results are presented for each measuring campaign in chronological order and are then additionally divided by GHG, starting with CO_2, and continuing with CH_4 and N_2O. As the differences in GHG concentrations between the mussel farms and their control sites are the focus of this study, the potential statistically significant differences between the corresponding data sets are the most central point of the results.

3.1. Continuous in situ measurements

In situ measurements of the surface water greenhouse gas concentrations were only performed during the second and third measuring campaign, in October 2023 and February 2024, since the necessary equipment was not available for the first campaign in September 2023.

3.1.1. Carbon dioxide (CO_2)

3.1.1.1. Second campaign (October 2023)

In situ measurements of CO_2 concentrations in the surface water for the second measuring campaign in October 2023 are presented in Figure 4 with a median concentration of 514±25 µatm around the farm in area A, and 529±7 µatm around the corresponding control site. The difference is deemed to be statistically significant with a P-value of <0.0001. Compared to area A the median concentrations were higher in area B and were measured to be 536±29 µatm around the farm and 532±11 µatm around the control site. The P-value is 0.0005, and the difference is statistically significant.

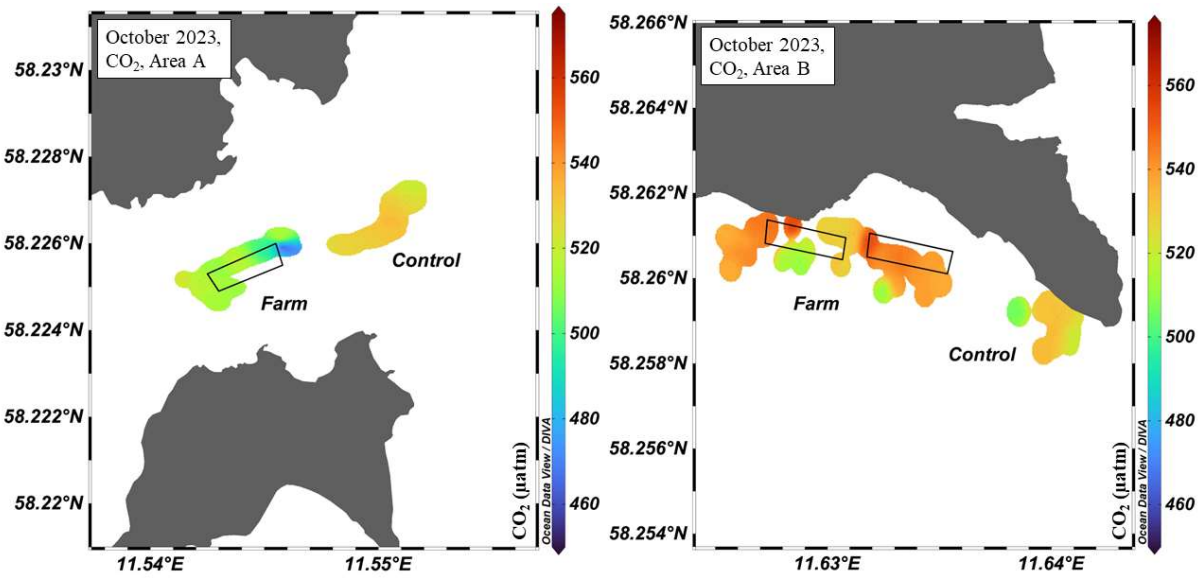

P-value	<0.001
Median Farm	513.647 µatm
Median Control	528.666 µatm

P-value	0.005
Median Farm	536.017 µatm
Median Control	532.101 µatm

Figure 4 Maps representing the measured concentrations of CO_2 at farm A (left) and farm B (right), together with the control sites, for the second campaign. The median values and P-values are shown below the maps. The black polygons represent the position of the mussel farms.

3.1.1.2. Third Campaign (February 2024)

Our findings show median CO_2 concentrations of 498±52 µatm at the farm in area A, and 499±1. µatm at the control site in area A for the in-situ surface measurements during the third campaign (Figure 5). There is a statistically significant difference with a P-value of 0.034. There was no statistically significant difference between farm and control in area B. The median concentrations 495±11 µatm around the farm and 496±20 µatm around the control site. The P-value is 0.053.

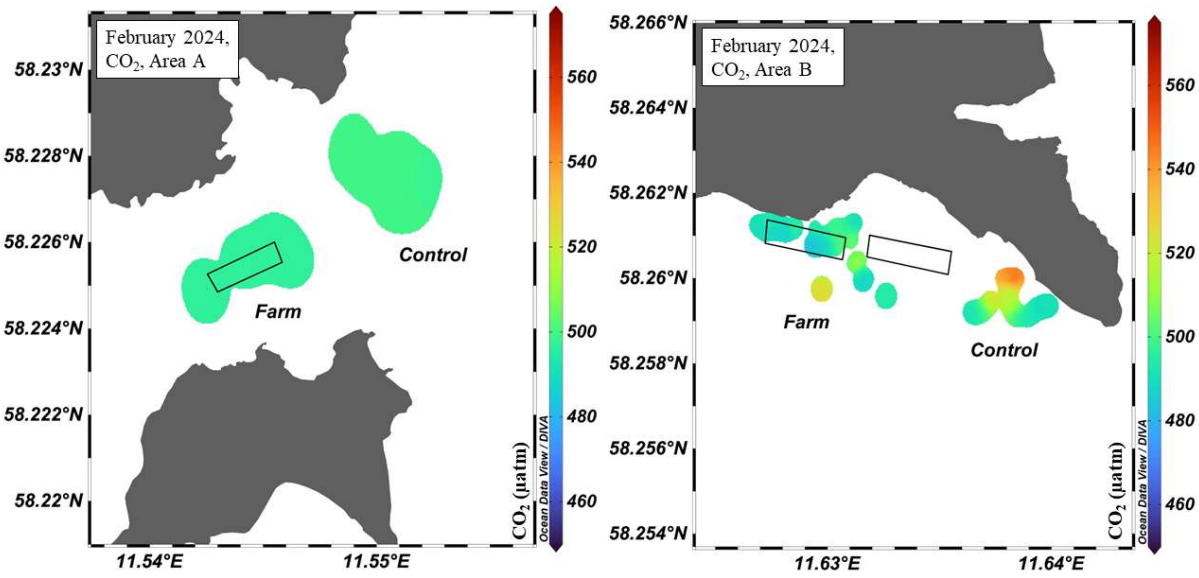

P-value	0.034
Median Farm	497.696 µatm
Median Control	498.626 µatm

P-value	0.053
Median Farm	494.699 µatm
Median Control	495.884 µatm

Figure 5 Maps representing the measured concentrations of CO_2 at farm A (left) and farm B (right), together with the control sites, for the third campaign. The median values and P-values are shown below the maps. The black polygons represent the position of the mussel farms.

3.1.2. Methane (CH_4)

It was decided to report the methane concentration from the continuous in situ measurements, but these numbers should be taken with caution. This is because the CH_4 concentrations that were recorded in situ were substantially lower than those generated from the discrete sampling. However, to compare trends, we retain these measurements valid. More details about this can be found in the Discussion section of this work.

3.1.2.1. Second campaign (October 2023)

CH_4 concentrations in the surface water had a median value of 5.0±0.7 nM at the farm and 5.0±0.4 nM at the control in area A for the second campaign. There is a statistically significant difference with a P-value of 0.033. In area B the concentrations were slightly higher and were measured to be 5.4±1.2 nM at the farm and 6.0±0.7 nM at the control site. A statistically significant difference is present with a P-value of 0.002. A graphical illustration of this can be found in Figure 6.

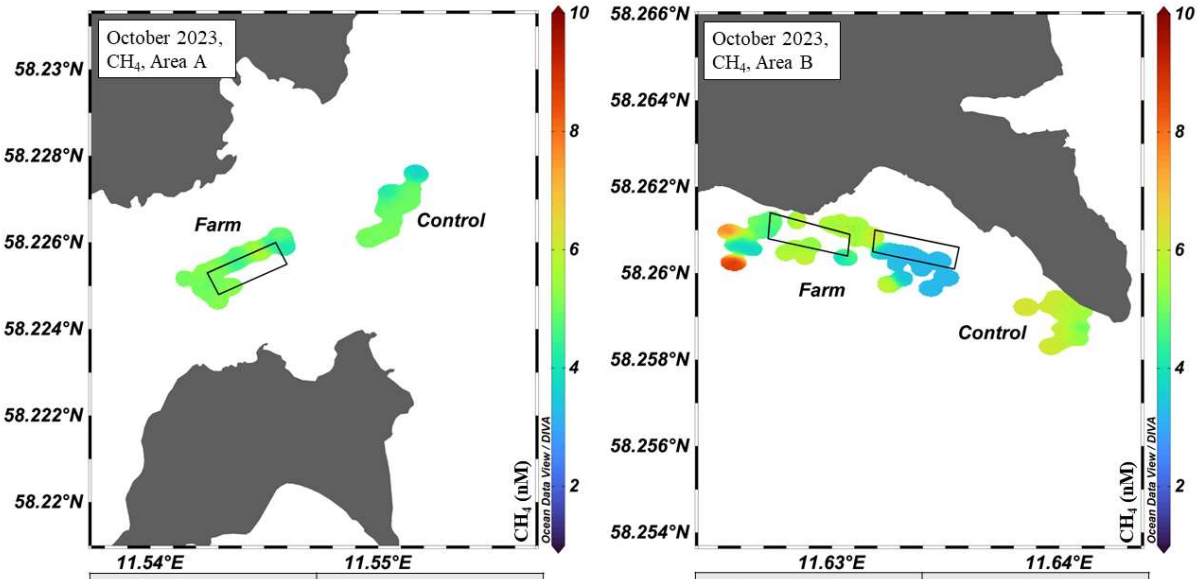

P-value	0.033
Median Farm	5.044 nM
Median Control	5.036 nM

P-value	0.002
Median Farm	5.357 nM
Median Control	5.991 nM

Figure 6 Maps representing the measured concentrations of CH_4 at farm A (left) and farm B (right), together with the control sites, for the second campaign. The median values and P-values are shown below the maps. The black polygons represent the position of the mussel farms.

3.1.2.2. Third campaign (February 2024)

Figure 7 represents the in-situ surface measurements of CH_4 for the third campaign. Median values were 4.8±0.5 nM for the farm and 4.8±0.0 nM for the control in area A. The p-value is 0.030 and the difference is statistically significant. In area B the median values were 4.8±0.3 nM at the farm and 4.8±0.1 nM at the control. No significant difference was found.

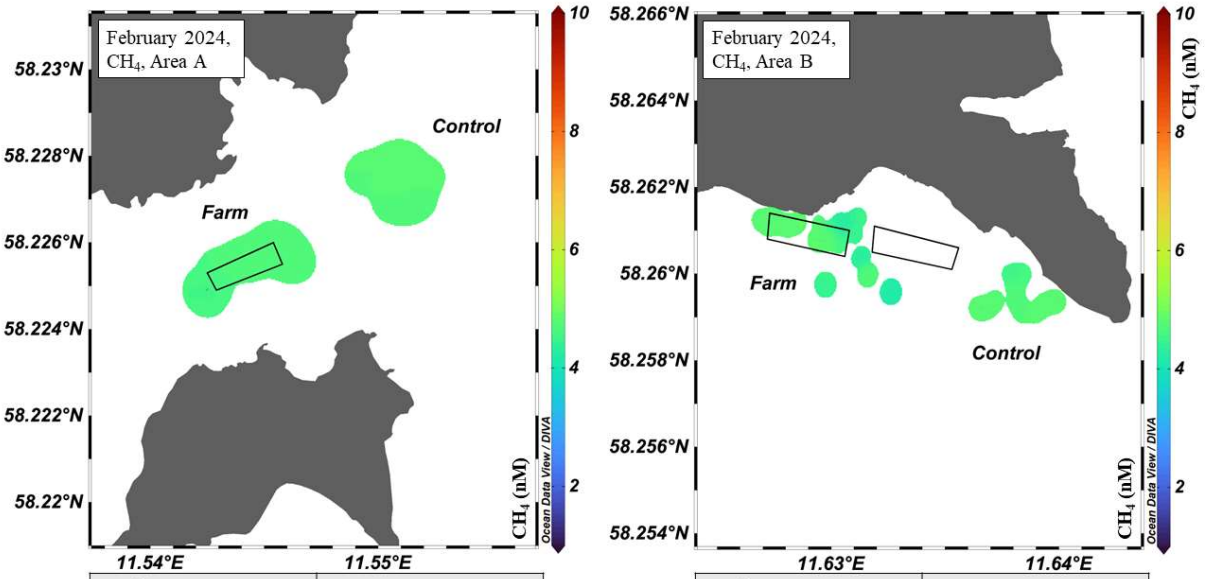

P-value	0.030
Median Farm	4.759 nM
Median Control	4.766 nM

P-value	0.251
Median Farm	4.755 nM
Median Control	4.775 nM

Figure 7 Maps representing the measured concentrations of CH_4 at farm A (left) and farm B (right), together with the control sites, for the third campaign. The median values and P-values are shown below the maps. The black polygons represent the position of the mussel farms.

3.1.3. Nitrous oxide (N_2O)

3.1.3.1. Second campaign (October 2023)

The surface water concentrations of N_2O for the second campaign presented in Figure 8 show statistically significant differences for both area A and area B, with p-values for 0.009 for A and <0.001 for B. Median concentrations were 12.1±0.4 nM for farm A and 12.2±0.0 nM for its control. The median farm concentration for area B was lower than in area A, at 11.1±0.8 nM, while the median control concentration for area B was 10.8±0.1 nM.

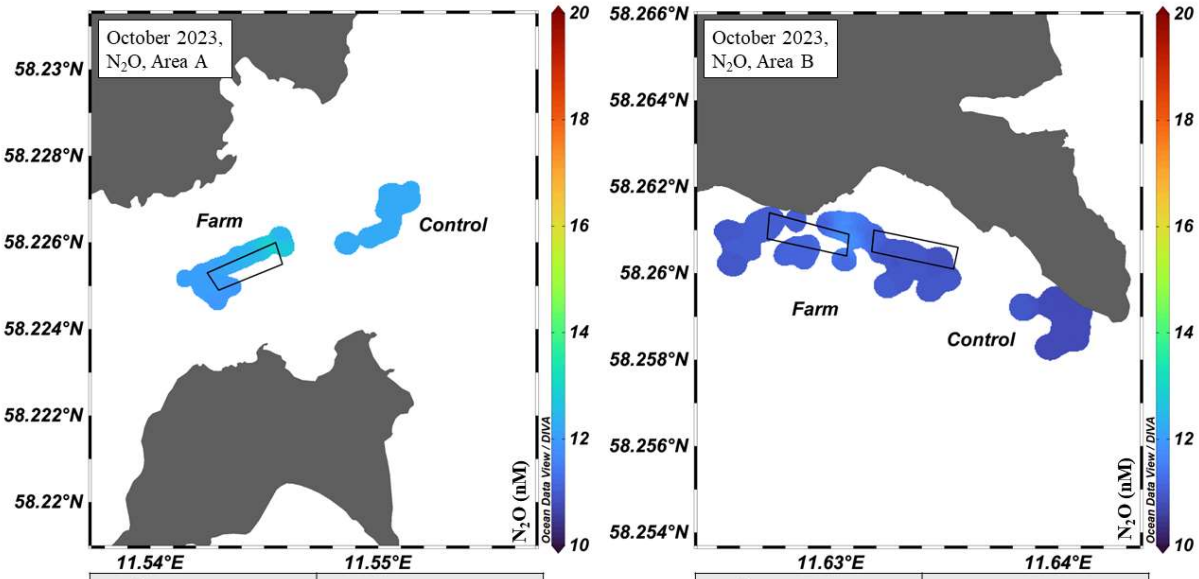

P-value	0.009
Median Farm	12.126 nM
Median Control	12.221 nM

P-value	<0.001
Median Farm	11.056 nM
Median Control	10.795 nM

Figure 8 Maps representing the measured concentrations of N_2O at farm A (left) and farm B (right), together with the control sites, for the second campaign. The median values and P-values are shown below the maps. The black polygons represent the position of the mussel farms.

3.1.3.2. Third campaign (February 2024)

Concentrations of surface N_2O were higher for the third campaign in comparison to the second campaign. The differences are deemed to be statistically significant for both areas. The median concentration for the farm in area A was 15.7±0.8 nM and 15.7±0.0 nM for its control site, and the p-value was 0.011. For area B, the farm's median concentration was 15.8±0.1 nM, and 15.8±0.3 nM for the control. The p-value for area B was 0.004. The overview is presented in Figure 9.

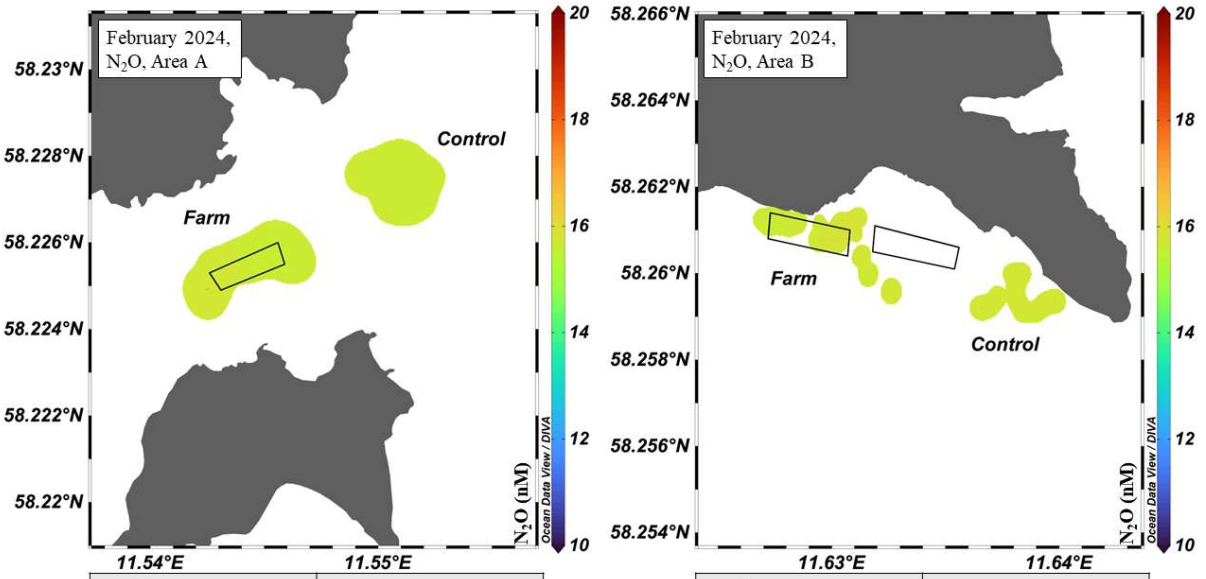

P-value	0.011
Median Farm	15.739 nM
Median Control	15.718 nM

P-value	0.004
Median Farm	15.819 nM
Median Control	15.769 nM

Figure 9 Maps representing the measured concentrations of N_2O at farm A (left) and farm B (right), together with the control sites, for the third campaign. The median values and P-values are shown below the maps. The black polygons represent the position of the mussel farms.

3.2. Discrete samples

The discrete samples were collected at each farm and control site (AF, AC, BF & BC), at three different depths (0.7-0.8 m, 5 m & 10 m) and during each of the three measuring campaigns (September 2023, October 2023 & February 2024). Here the concentrations of the following compounds were analyzed: dissolved inorganic carbon (DIC), CH_4 & N_2O.

The results of the discrete sampling analysis are presented in three arrays of graphs, one array for each compound, where each graph shows the concentrations of the measured compound at the chosen depths at each site for each campaign. The individual graphs also include data from the conductivity, temperature, depth (CTD) measurement at the relevant site. This data provides us with the site's oxygen (blue) and salinity (grey) concentration, as well as water temperature (black). While each array of plots focuses on one of the three studied compounds (Figure 10-12), conductivity, salinity and temperature do not differ between the arrays, since they represent the same spatial and temporal parameters.

3.2.1. CTD-data (oxygen, salinity, and temperature)

3.2.1.1 Oxygen

The oxygen concentrations in the water column for the September 2023 campaign range from 100 µM to 257 µM. The concentrations decreased with depth. Average values were 199±43 µM for the farm in area A and 189±41 µM for the control. 203±44 µM and 202±49 µM represent the average oxygen concentrations for farm and control in area B.

Concentrations of oxygen for October 2023 varied less than in the first campaign. They varied between 238 µM and 306 µM. For area A, they decreased slightly with depth, while they stayed

almost completely unchanged throughout the water column in area B. The collected average concentrations of oxygen were 281±14 µM, 273±7 µM, 254±2 µM and 253±1. µM for farm A, control A, farm B and control B respectively.

During the final measuring campaign in February 2024, the highest oxygen concentrations were recorded. These ranged from 323 µM to 380 µM. While the concentrations did not vary much throughout the water column in the surface and middle water, a decrease was observed at around eight meters. The averages were 374±1 µM for the farm in area A and 360±18 µM for the control. For area B the averages were 371±5 µM for the farm and 361±14 µM for the control site. The oxygen concentrations for all sites and all campaigns are presented in Figures 10-12.

3.2.1.2. Salinity

The lowest levels of salinity that were recorded in this study were observed in the first campaign in September 2023. The range of salinity across all four sites for this campaign was between 21 PSU and 24 PSU. The lower levels were present in the surface water. A steady increase took place at a depth of four to five meters. The peak levels of salinity for this campaign were all found in the bottom of the water column. Averages for area A were 22±0.6 PSU at the farm and 22±0.7 PSU at the control site. For area B the average values were 22±0.8 PSU at the farm site and 22±0.9 PSU at the control site.

The salinity throughout the water column was less varied for the second campaign, when compared to the first, the most dominant in area B. The lowest recorded level of salinity during the October campaign was 21 PSU and the highest was 26 PSU. 22±0.1 PSU, 23±1.4 PSU, 22±0.0 PSU and 22±0.1 PSU represent the averages for area A farm and control and area B farm and control.

Campaign three in February 2024 included the highest levels of salinity in the water column. recorded during this study. The observed range was from 23.232 PSU to 25.598 PSU. Throughout the water column the salinity was mostly unchanged until a depth of around nine meters where an increase could be observed. The average salinity at the farm in area A was 23±0.0 PSU and 24±0.5 PSU at the control site. For the farm at area B there was an average salinity of 24±0.1 PSU, it was the same at the control area. The salinity for all sites and all campaigns is presented in Figures 10-12.

3.2.1.3. Temperature

Water temperatures for the measuring campaign in September 2023 ranged from 17.1˚C to 18.3˚C. The lowest temperatures were found at the deepest depths, while the highest temperatures were recorded at the surface water. This holds true for all four sites. Temperatures declined drastically around a depth of 5 to 7 meters. The average water temperature was measured to be 17.9±0.2 ˚C at the farm and 17.8±0.3 ˚C at the control site in area A. For Area B the average temperature was 18.1±0.3 ˚C, both at the farm and the control.

Temperatures were lower in October 2023, compared to the previous campaign, ranging from 7.6˚C to 10.5˚C, however, in contrast to the September campaign, the lowest temperatures were measured in the surface water at area A. The highest temperatures were recorded in area B. Here the water column was almost completely homogenous, and no clear difference in

temperature was visible. Average temperatures were 8.2±0.2˚C at farm A, 8.2±0.4˚C at control A, 10.3±0.1˚C at farm B and 10.3±0.1˚C at control B.

The February 2024 campaign exhibited the lowest water temperatures in this study, with the lowest recorded temperature being 0.6˚C and peaking at 2.3˚C. Temperatures did not change meaningfully until a depth of around 8 meters, after which they increased. At area A the average temperatures were 0.8±0.0˚C for the farm and 1.0±0.4˚C for the control. 0.8±0.2˚C was the average water temperature for the farm in area B and 0.9±0.2˚C for the control. The temperatures for all sites and all campaigns are presented in Figures 9-11.

3.2.2. Dissolved inorganic carbon (DIC)

For the first measuring campaign, the DIC concentrations at both farms and both controls did not show any statistically significant differences in the surface water (*September 23* in Figure 10). Amongst the data collected from the middle depth, only the control site in area A showed a statistically significantly higher concentration of DIC. At the bottom depth, both control sites had concentrations of DIC that were statistically significantly higher than their farm sites. During the second campaign none of the measured concentrations of DIC showed any statistically significant differences when farm and control site were compared (*October 2023* in Figure 10).

In February 2024, for the final campaign, one statistically significant difference in DIC concentration was found in the surface water (*February 2024* in Figure 9). It is the farm in area B that showed this statistically significantly higher concentration. Significant differences were also found in the middle, here the controls had statistically significantly higher concentrations of DIC than the farms. The same was observed for the bottom concentrations.

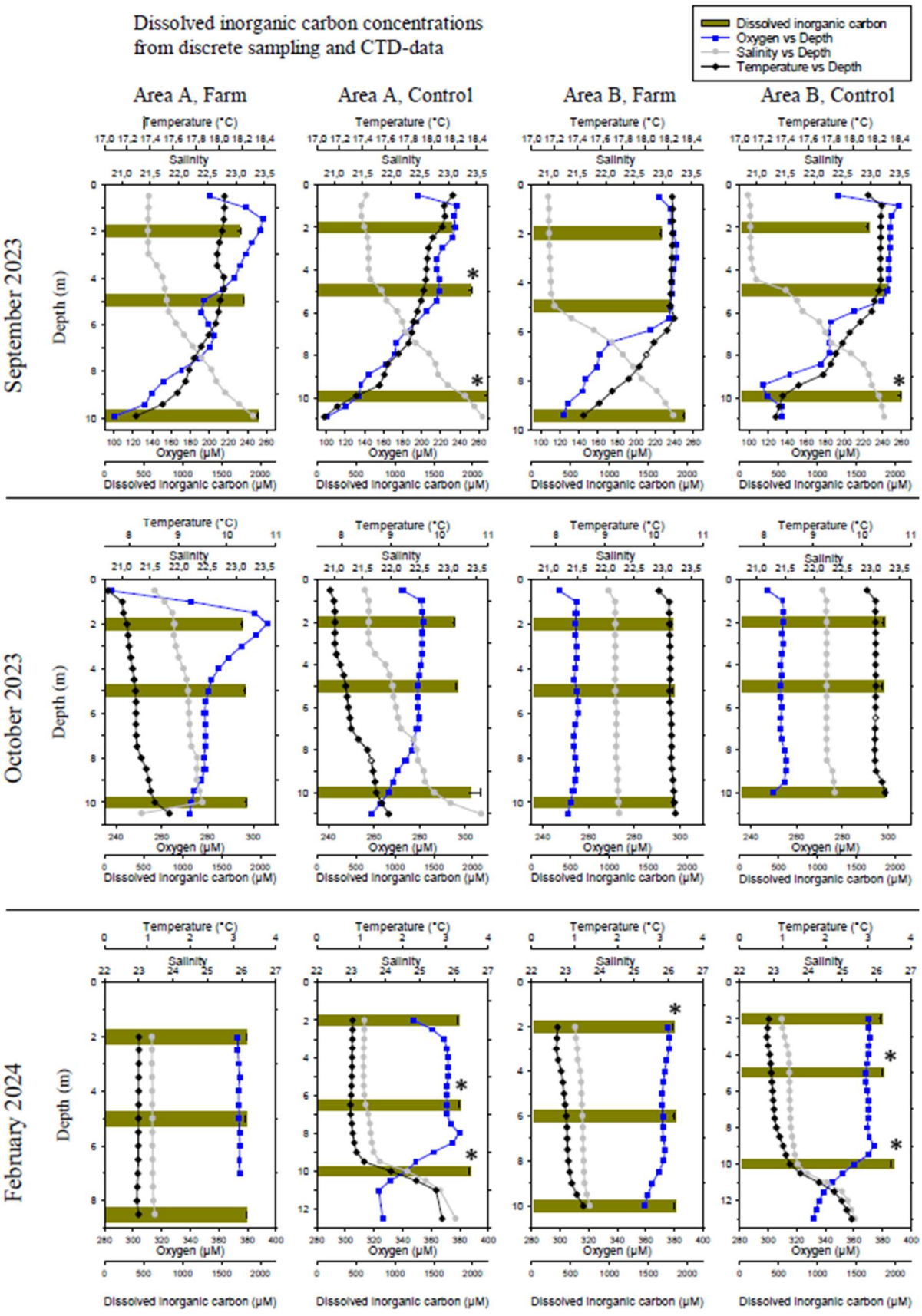

Figure 10 An array of plots showing the concentrations of DIC at the chosen depths for each campaign (horizontal) and each site (vertical). The * marks concentrations that show a statistical significantly higher value compared to their farm or control site. Each plot has one Y-axis (depth) and four X-axis (temperature, salinity, oxygen, DIC).

3.2.3. Methane (CH_4)

As shown in Figure 11, no statistically significant differences between the CH_4 concentrations at the farm and the control sites were found in the surface water or in the middle of the water column during the first campaign. The only concentration that was deemed to be higher in a statistically significant way, when compared to its counterpart, was in the bottom water of the farm in area A (*September 2023* in Figure 11).

The second campaign could only show one instance of statistically significant difference in CH_4 concentration between farm and control. Here the higher concentration was observed at the bottom of the farm site in area B (*October 2023* in Figure 11).

For February 2024 there were two comparisons between farm and control that showed a statistically significant difference. In one of these cases the higher concentration was in the bottom water of the control site in area A, and the other one was the surface water at the control in area A (*February 2024* in Figure 11).

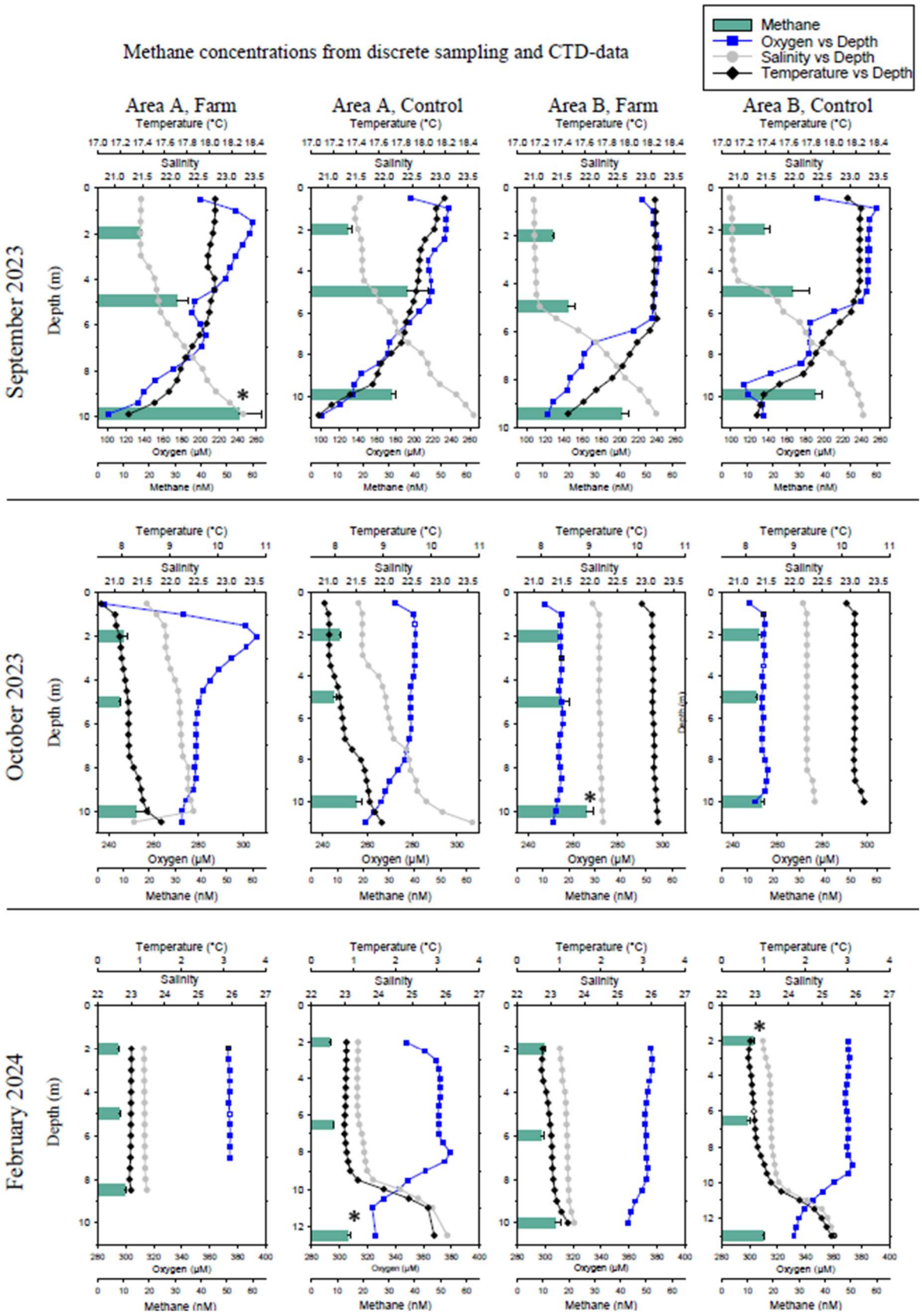

Figure 11 An array of plots showing the concentrations of CH_4 at the chosen depths for each campaign (horizontal) and each site (vertical). The * marks concentrations that show a statistical significantly higher value compared to their farm or control site. Each plot has one Y-axis (depth) and four X-axis (temperature, salinity, oxygen, CH_4).

3.2.4. Nitrous oxide (N_2O)

The discrete sampling analysis of N_2O has identified only a single case of difference between a farm and control which was deemed significant (*February 2024* in Figure 12). The higher concentration was found in the bottom water of the farm at area A, in comparison to the control site. At all other depths no difference was found between the farms and the controls.

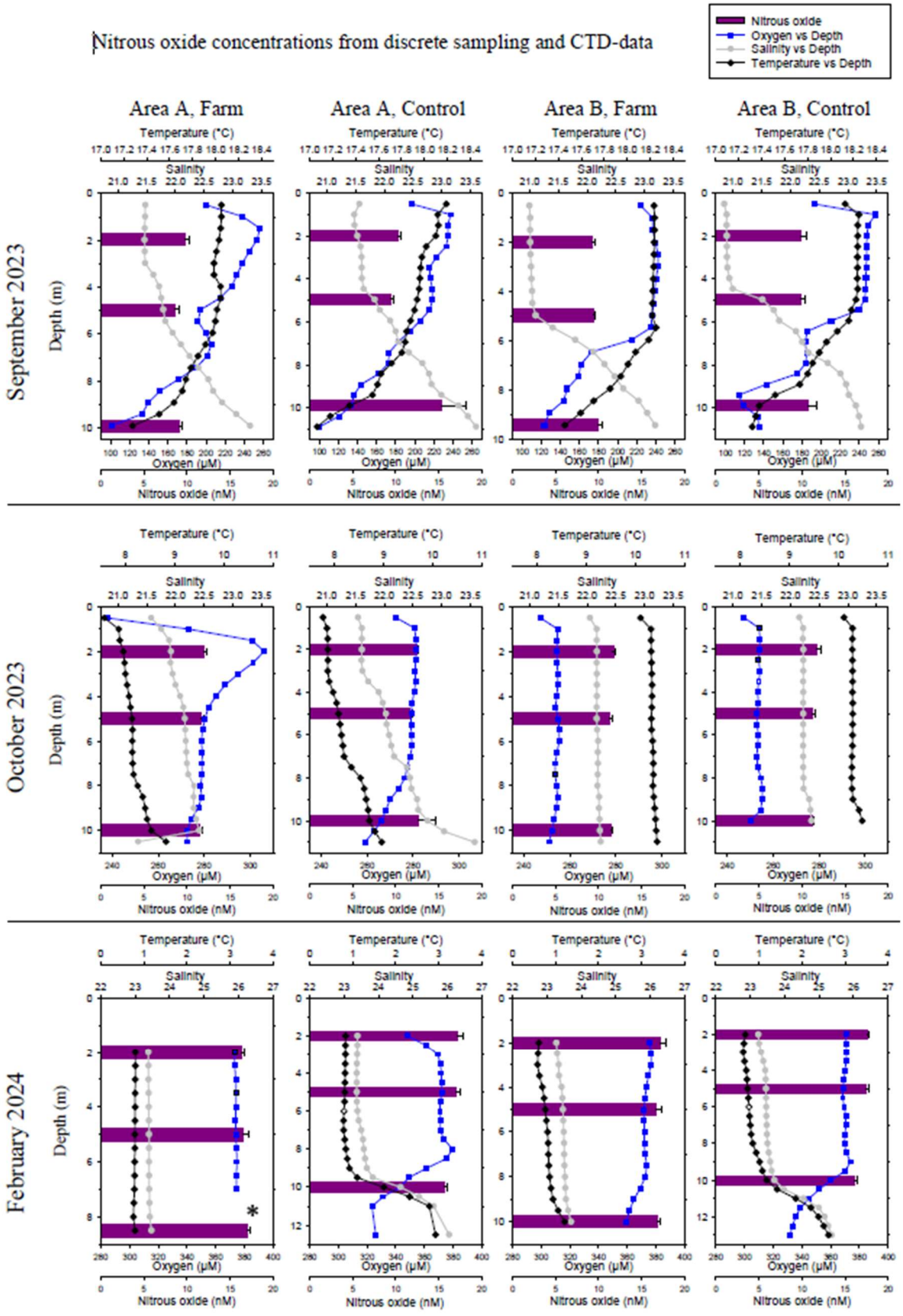

Figure 12 An array of plots showing the concentrations of N_2O at the chosen depths for each campaign (horizontal) and each site (vertical). The * marks concentrations that show a statistical significantly higher value compared to their farm or control site. Each plot has one Y-axis (depth) and four X-axis (temperature, salinity, oxygen, N_2O).

4. Discussion

The aim of this study was to analyze the impact of mussel farming on the emissions and inventories of CO_2, CH_4 and N_2O from seawater in comparison to the control areas unaffected by aquaculture. The focus was not on the ecological and physiological mechanisms of mussel respiration.

4.1. Carbon dioxide and dissolved inorganic carbon (CO_2 & DIC)

In situ measurements in October showed a significantly higher CO_2 concentration at the control site in area A, however, there was also a significantly higher concentration at the farm in area B. This reverse trend between the two study areas, combined with the fact that even the statistically significant differences, are still relatively low (less than 1%), seems to indicate the mussel farms do not contribute to generally higher CO_2 concentrations. This is interesting in the context of other studies such as Tamburini et al., 2022, who found via the use of life cycle assessment (LCA), that mussel farming in the Mediterranean Sea can be considered a net carbon sink. The farming of other types of bivalves, like clams and oysters, has also been shown to have a negligible impact on CO_2 emissions (Ray et al., 2019; Tamburini et al., 2022). For the post-harvest campaign in February 2024, the in-situ measurements show significantly higher surface water CO_2 concentrations only at one of the control areas, which is surprising since most mussels had been removed by this point, and no differences were expected. A visual summary of the results from the in-situ measurement analysis for all the studied GHGs can be found in Figure 13.

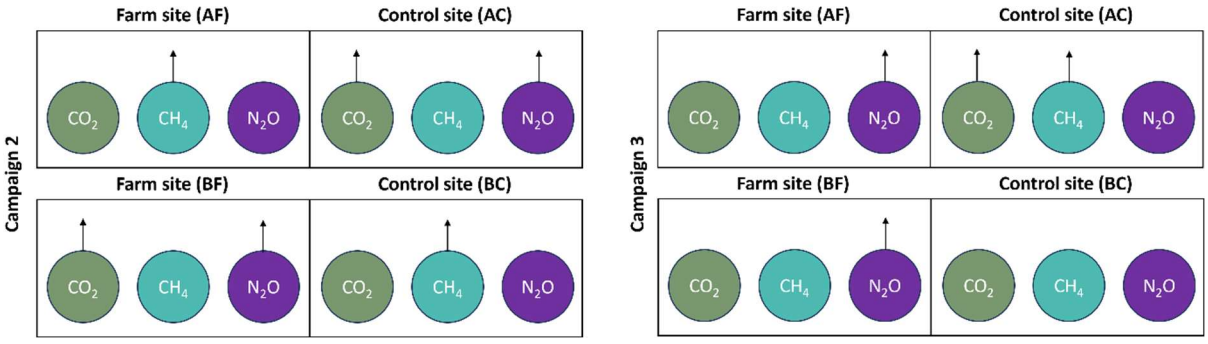

Figure 13 Graphical summary of the in-situ measurements results of the studied GHGs during campaign 2 (left) and campaign 3 (right) in the farm and control areas. Measurements with a significantly higher concentration are denoted with an upwards arrow.

The discrete sampling analysis of DIC for the first campaign only showed significantly higher concentrations in the control sites. Regardless, this cannot lead to higher emissions, since these differences are found only in the middle and bottom of the water column, while the surface concentrations remained similar between farms and controls. This is important to be noted as only the surface water layer contributes to sea-to-air fluxes of greenhouse gases. During the second campaign, discrete sampling showed no significantly higher concentrations at any of the studied sites. This in turn means that no increased emissions from the mussel farms can be pointed out by this analysis. When it comes to the third campaign in February 2024 there is only one instance of significantly higher concentration of DIC in the surface water. This is at the farm in area B. This is very surprising as these data were collected after the harvest of the

mussel farm, and it could suggest that carbon dynamics in the study area are dominated by other factors, such as off-shelf transportation of dissolved carbon into the open ocean (Bourgeois et al., 2016), or biological carbon fixation, enhanced by anthropogenic nutrient inputs (Lacroix et al., 2021) to such a degree that the presence or absence of large amounts of blue mussels pales in comparison. While the data from the in-situ measurements are not consistent between all the study areas and do not show clearly higher or lower concentrations for the impacted areas or the controls, the data from the discrete sampling from the first two campaigns (pre harvest) showed no significant changes in the surface concentrations between farms and controls. DIC is a substrate for bivalve shell formation, since mussels use carbonate (CO_3^{2-}) and bicarbonate (HCO_3^-) to form the calcium carbonate ($CaCO_3$) for their shells (Marin et al., 2007; McDougall and Degnan, 2018). Interestingly, the lower concentrations of DIC in the middle and bottom water at the farm sites would suggest that the presence of mussels can absorb DIC, potentially to be used for the process of the mentioned shell formation (Marin et al., 2007; McDougall and Degnan, 2018). Additionally, mussels and other shell-forming bivalves emit CO_2 through respiration (Stief et al., 2009), and thereby contribute to DIC. However, through the aforementioned formation of shells and the binding of CO_3^{2-} and HCO_3^-, blue mussels and other bivalves could have a net negative effect on DIC concentrations (Tamburini et al., 2022), or at least a neutral effect where their emissions and their sequestration of DIC balance each other out (Lee et al., 2024).

4.2. Methane (CH_4)

All methane concentrations that were measured with the trace gas analyzers for the in-situ data collection during this study show surface water concentrations that are lower than expected from the discrete samples analyzed by GC. They are approximately 25% of the concentrations that were recorded with the discrete sampling method. This could be caused by a design flaw or a weakness in the system that pumps the seawater into the spray chamber. Another possible explanation could be the chemical properties of CH_4, since it has no covalent bonds and is thus hydrophobic (Yamamoto et al., 1976), in contrast to CO_2 and N_2O, which are more easily dissolved in seawater (Weiss, 1974; Weiss and Price, 1980). This could lead to considerably less CH_4 reaching the trace gas analyzers. A more likely explanation could be that the flow rate of the pump for the closed loop system was too high. Brown et al., 2023 compares a continuous closed loop measuring system for CH_4 dissolved in seawater with a more established discrete sampling and GC-analysis method. According to them, the results of the two systems are comparable. However, they described a lower flow rate for the measurement of CH_4 (0.072 m^3/h) compared to the one used in this study. This could be explained by the low solubility of CH_4 which means that it needs a longer residence time to reach full equilibration. The choice to still include this data was based on the assumption that they would still be valid for the comparison between the mussel farms and the control sites, even if they do not resemble the actual concentrations of CH_4.

When it comes to the in-situ measurements of CH_4, I expected higher concentrations at the farms during the second campaign (pre harvest) and no significant differences during the third campaign (post-harvest). Recorded concentrations were indeed higher for the farm in area A for the second campaign but surprisingly they showed the opposite trend in area B, which renders

the data somewhat unclear and hard to interpret. For the third campaign, there were no significantly higher CH_4 concentration at the farms, but the control in area A. Noticeably higher methane concentrations at the mussel farms, even after the harvest, would have been expected as the sedimentation rates under long line mussel farms have been seen to be 100% to 200% higher compared to areas without farms (Dahlbäck and Gunnarsson, 1981; Grant et al., 1995), and CH_4 production in sediments can be increased by higher organic matter loading (Egger et al., 2016). This loading of organic matter can be further enhanced by the deposition of feces in the sediment underneath the aquaculture (Fulweiler et al., 2007). However, some bivalves are known to be able to consume CH_4 (Childress et al., 1986), so the potential increase in methane released from loaded sediment could be balanced out by this dynamic. Once we take the results of the discrete sampling from the second and third campaign and the associated CTD-data into account, which shows a very mixed and flushed water column, it becomes more likely that the registered differences from the in situ measurement are within the natural difference caused by other factors, and that whatever impact the mussel farms may have on the local methane dynamics, it is too insignificant to be recorded. Analysis of the discrete sampling did not show a single incident of significantly higher concentration of CH_4 in the surface water at any of the farm sites. This leads us to believe that mussel farming does not enhance atmospheric CH_4 emissions. Additionally, I could observe that CH_4 is dependent on oxygen concentrations, as shown in Figure 14, with the highest CH_4 concentrations, and lowest oxygen concentrations being recorded in the bottom water during stratified water column conditions. This is in line with the basics of methanogenesis in marine environments (Lyu et al., 2018).

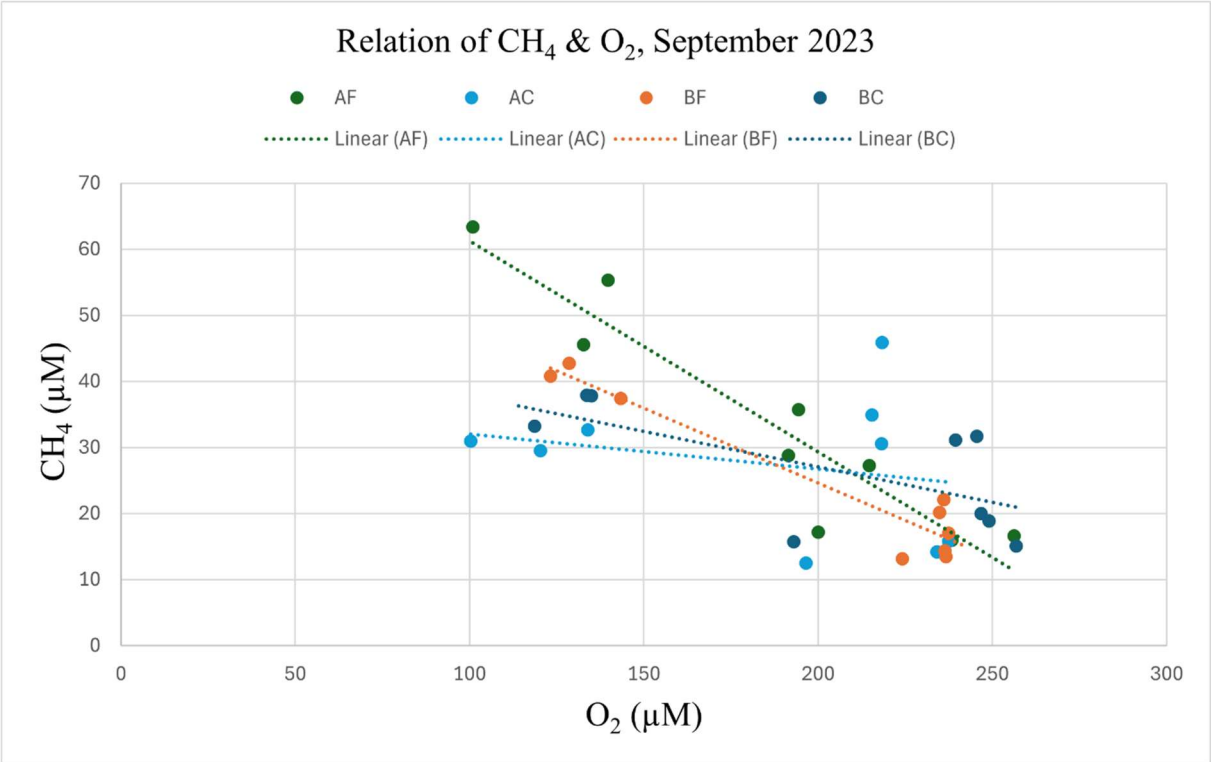

Study area	Equation	R^2
A Farm (AF)	Y = -0.3 X + 93.2	0.9
A Control (AC)	Y = -0.1 X + 37.3	0.1
B Farm (BF)	Y = -0.2 X + 69.9	0.9
B Control (BC)	Y = -0.1 X + 48.6	0.4

Figure 14 Regression analysis showing the connection between decreasing O_2 concentrations and higher CH_4 concentrations for the first campaign in September 2023. This figure includes all four study areas: Farm A (AF) is represented by green markers, Control A (AC) by light blue ones, Farm B (BF) by orange ones and Control C (BC) is represented by dark blue markers. Associated R^2 values and equations for the regression analysis shown in the table below.

4.3. Nitrous oxide (N_2O)

As observed for the in-situ measurements of CO_2 and CH_4 during the second campaign, the same contrasting results were observed for N_2O. Again, I could observe a seemingly reversed trend between area A and area B, with a significantly higher concentration at the control in area A, and a significantly higher concentration at the farm in area B, which in turn leads to the assumption that the in-situ results for the second campaign were influenced by other factors such as unclassified sources or sinks of N_2O in the area and discharge or distribution of the water masses. Thus, the recorded differences, statistically significant or not, should not be attributed to the mussel farms. A visual summary of the results from the in-situ measurement analysis for all the studied GHGs can be found in Figure 13. Some have described the aquaculture of bivalves such as the blue mussel as an effective measures to combat eutrophication (Kotta et al., 2020), and it could thus be considered to indirectly lower local N_2O emissions by reducing available nutrients in the water, since bivalves are filter feeders

(Crawford et al., 2003). However, other studies have described that areas with a high density of blue mussels, like aquacultures, can be major contributors to local N_2O dynamics and emissions (Voet et al., 2023). An interesting aspect of these potential emissions is that the majority of N_2O produced by blue mussels was found to come from the microbial biofilm situated on the outside of the animals' shell and not in the gut of the mussels (Heisterkamp et al., 2013). For the third campaign both farms showed a significantly higher N_2O concentration than their control areas. This is interesting since the mussels had been harvested at the time of the measurements, and one would instinctually expect that the GHG concentrations would be much lower. However, the harvest of the farms was conducted only a few days before the measurement (A. Granhed, personal communication, February 12, 2024), and the physical activity during the harvesting has most likely led to the release of organic matter in the form of marine snow (Alldredge et al., 1993), which in turn could lead to an increase in N_2O production via nitrification and/or denitrification (Bonin et al., 2002). Analysis of the discrete samples did not show any significant differences in the surface water concentrations of N_2O, for any of the campaigns. Based on this water column data, one can assume that the mussel farms do not lead to an environmentally important increase in N_2O emissions to the atmosphere.

5. Opportunities and Limitations

A number of methodological challenges were identified during this project, but they can also present opportunities for the improvement of future studies that aim to investigate the complex dynamics of GHGs and aquaculture. The study confirmed that the discrete sample and GC-method can produce high quality data and provided valuable insights in how to optimize the in-situ measurements with the LI-COR analyzers, especially when it comes to the measuring of CH_4. The in-situ measurements for the second campaign showed opposite trends for all three studied compounds, and no direct connection between the in-situ measurements and the discrete surface water samples could be observed. One possible explanation for that could be the large discrepancies between the sample sizes of surface water discrete samples ($n = 3$) and the in-situ measurements ($13 \leq n \leq 165$) for all the studied gases. Increasing the sample size for discrete sampling could help reduce variation. Obtaining more datapoints in proximity of the farm and control sites during in situ measurements to get data sets of similar size and distribution to strengthen statistical analysis could also improve a future study with a similar focus. Choosing more easily accessible mussel farms and exercising more consideration for potential patterns of water flow and currents while choosing control sites would be advantageous. Additionally, close collaboration with the owners and operators of mussel farms is perhaps the most important aspect that was missing during this study. Getting as much information as possible about the age and the population of mussels, as well as the different farming techniques that are used could be extremely valuable for a study like this one. However, this can be difficult, as the interest of shareholders in mussel farming might not always align with scientific research focusing on potentially harmful environmental impacts.

6. Conclusion

This work aimed to answer the question if mussel farming has a negative impact on the emissions of the three major greenhouse gases and contributes negatively to global climate change. Lack of significant differences in surface levels of CO_2, CH_4 and N_2O would suggest that the impact of mussel farming on greenhouse gas emissions is negligible. In fact, there was high variability in concentrations of the three GHGs between campaigns, between sites, and between different water column depths. It shows that the system was affected by natural spatial and seasonal variability more than by the impact of the farmed mussels, both during pre- and post-harvest. The statistically significant differences between some of the measured surface concentrations are very likely not of environmental relevant.

The hypothesis, stated in the introduction, that GHG concentrations in the waters directly influenced by the mussel farms are higher compared to the concentrations at the non-impacted control areas, can thus not be confirmed.

7. Acknowledgments

First and foremost, I want to thank my supervisor Stefano Bonaglia for taking me on as a student and for guiding me through marine science, a completely new field for me. I also want to thank my co-supervisors Francisco Nascimento, Tobia Politi and Henry L. S. Cheung for all the help in the lab, the office and on board of *Alice.* In addition, I want to thank Yvonne Y. Y. Yau for all the times when she answered my questions. Formas Research Council and the Department of Marine Science at the University of Gothenburg deserve a lot of thanks for funding this project. Everyone at Kristineberg Center for Marine Research and Innovation also deserves my sincerest thanks, most of all the crew of R/V Alice, skippers Christian Thörnblom and Ursula Schwartz. Johanna Berggren and Maria Kaspersen also deserve my gratitude for all the help with my part-time employment and leave of absence. I also want to express a heartfelt ‘thank you’ to my family and friends for support in all nonscientific aspects of life. Most of all my partner Monika Malak deserves all the thanks in the world for the countless hours of unwavering support, insightful advice and pushing me when I wanted to stop.

8. Reference list

Alldredge, A.L., Passow, U., Logan, B.E., 1993. The abundance and significance of a class of large, transparent organic particles in the ocean. Deep Sea Res. Part Oceanogr. Res. Pap. 40, 1131–1140. https://doi.org/10.1016/0967-0637(93)90129-Q

Babinszky, L., Halas, V., W.A., M., 2011. Impacts of Climate Change on Animal Production and Quality of Animal Food Products, in: Kheradmand, H. (Ed.), Climate Change - Socioeconomic Effects. InTech. https://doi.org/10.5772/23840

Béné, C., Arthur, R., Norbury, H., Allison, E.H., Beveridge, M., Bush, S., Campling, L., Leschen, W., Little, D., Squires, D., Thilsted, S.H., Troell, M., Williams, M., 2016. Contribution of Fisheries and Aquaculture to Food Security and Poverty Reduction: Assessing the Current Evidence. World Dev. 79, 177–196. https://doi.org/10.1016/j.worlddev.2015.11.007

Bonaglia, S., Brüchert, V., Callac, N., Vicenzi, A., Chi Fru, E., Nascimento, F.J.A., 2017. Methane fluxes from coastal sediments are enhanced by macrofauna. Sci. Rep. 7, 13145. https://doi.org/10.1038/s41598-017-13263-w

Bonin, P., Tamburini, C., Michotey, V., 2002. Determination of the bacterial processes which are sources of nitrous oxide production in marine samples. Water Res. 36, 722–732. https://doi.org/10.1016/S0043-1354(01)00269-X

Borges, A.V., Delille, B., Frankignoulle, M., 2005. Budgeting sinks and sources of CO_2 in the coastal ocean: Diversity of ecosystems counts. Geophys. Res. Lett. 32, 2005GL023053. https://doi.org/10.1029/2005GL023053

Bourgeois, T., Orr, J.C., Resplandy, L., Terhaar, J., Ethé, C., Gehlen, M., Bopp, L., 2016. Coastal-ocean uptake of anthropogenic carbon. Biogeosciences 13, 4167–4185. https://doi.org/10.5194/bg-13-4167-2016

Brown, I.J., Kitidis, V., Rees, A.P., 2023. Simultaneous high-precision, high-frequency measurements of methane and nitrous oxide in surface seawater by cavity ring-down spectroscopy. Front. Mar. Sci. 10, 1197727. https://doi.org/10.3389/fmars.2023.1197727

Carlson, C.A., Bates, N.R., Hansell, D.A., Steinberg, D.K., 2001. Carbon Cycle, in: Encyclopedia of Ocean Sciences. Elsevier, pp. 477–486. https://doi.org/10.1016/B978-012374473-9.00272-1

Childress, J.J., Fisher, C.R., Brooks, J.M., Kennicutt, M.C., Bidigare, R., Anderson, A.E., 1986. A Methanotrophic Marine Molluscan (Bivalvia, Mytilidae) Symbiosis: Mussels Fueled by Gas. Science 233, 1306–1308. https://doi.org/10.1126/science.233.4770.1306

Crawford, C.M., Macleod, C.K.A., Mitchell, I.M., 2003. Effects of shellfish farming on the benthic environment. Aquaculture 224, 117–140. https://doi.org/10.1016/S0044-8486(03)00210-2

Dahlbäck, B., Gunnarsson, L.Å.H., 1981. Sedimentation and sulfate reduction under a mussel culture. Mar. Biol. 63, 269–275. https://doi.org/10.1007/BF00395996

Doney, S.C., Fabry, V.J., Feely, R.A., Kleypas, J.A., 2009. Ocean Acidification: The Other CO_2 Problem. Annu. Rev. Mar. Sci. 1, 169–192. https://doi.org/10.1146/annurev.marine.010908.163834

Dore, J.E., Lukas, R., Sadler, D.W., Church, M.J., Karl, D.M., 2009. Physical and biogeochemical modulation of ocean acidification in the central North Pacific. Proc. Natl. Acad. Sci. 106, 12235–12240. https://doi.org/10.1073/pnas.0906044106

Egger, M., Lenstra, W., Jong, D., Meysman, F.J.R., Sapart, C.J., Van Der Veen, C., Röckmann, T., Gonzalez, S., Slomp, C.P., 2016. Rapid Sediment Accumulation Results in High Methane Effluxes from Coastal Sediments. PLOS ONE 11, e0161609. https://doi.org/10.1371/journal.pone.0161609

EPA, 2023. Inventory of U.S. Greenhouse Gas Emissions and Sinks: 1990-2021.

FAO, 2024. Mytilus edulis. Cultured Aquatic Species Information Programme. Text by Goulletquer, P., In: Fisheries and Aquaculture. Rome. [WWW Document]. URL https://www.fao.org/fishery/en/culturedspecies/mytilus_edulis/en (accessed 4.30.24).

FAO (Ed.), 2022. Towards blue transformation, The state of world fisheries and aquaculture. FAO, Rome. https://doi.org/10.4060/cc0461en

Fennel, K., Testa, J.M., 2019. Biogeochemical Controls on Coastal Hypoxia. Annu. Rev. Mar. Sci. 11, 105–130. https://doi.org/10.1146/annurev-marine-010318-095138

Freitas, B., Delagran, L., Griffin, E., Miller, K.L., Hirschfield, M., 2008. Too Few Fish: A Regional Assessment of the World's Fisheries.

Fry, J.M., 2012. Carbon Footprint of Scottish Suspended Mussels and Intertidal Oysters.

Fulweiler, R.W., Nixon, S.W., Buckley, B.A., Granger, S.L., 2007. Reversal of the net dinitrogen gas flux in coastal marine sediments. Nature 448, 180–182. https://doi.org/10.1038/nature05963

Gerber, P.J., Hristov, A.N., Henderson, B., Makkar, H., Oh, J., Lee, C., Meinen, R., Montes, F., Ott, T., Firkins, J., Rotz, A., Dell, C., Adesogan, A.T., Yang, W.Z., Tricarico, J.M., Kebreab, E., Waghorn, G., Dijkstra, J., Oosting, S., 2013. Technical options for the mitigation of direct methane and nitrous oxide emissions from livestock: a review. Animal 7, 220–234. https://doi.org/10.1017/S1751731113000876

Gorissen, S.H.M., Witard, O.C., 2018. Characterising the muscle anabolic potential of dairy, meat and plant-based protein sources in older adults. Proc. Nutr. Soc. 77, 20–31. https://doi.org/10.1017/S002966511700194X

Grant, J., Hatcher, A., Scott, D.B., Pocklington, P., Schafer, C.T., Winters, G.V., 1995. A Multidisciplinary Approach to Evaluating Impacts of Shellfish Aquaculture on Benthic Communities. Estuaries 18, 124. https://doi.org/10.2307/1352288

Hansson, D., Stigebrandt, A., Liljebladh, B., 2013. Modelling the Orust fjord system on the Swedish west coast. J. Mar. Syst. 113–114, 29–41. https://doi.org/10.1016/j.jmarsys.2012.12.003

Heisterkamp, I.M., Schramm, A., Larsen, L.H., Svenningsen, N.B., Lavik, G., De Beer, D., Stief, P., 2013. Shell biofilm-associated nitrous oxide production in marine molluscs: processes, precursors and relative importance. Environ. Microbiol. 15, 1943–1955. https://doi.org/10.1111/j.1462-2920.2012.02823.x

Hoegh-Guldberg, O., Bruno, J.F., 2010. The Impact of Climate Change on the World's Marine Ecosystems. Science 328, 1523–1528. https://doi.org/10.1126/science.1189930

Hofmann, M., Schellnhuber, H.-J., 2009. Oceanic acidification affects marine carbon pump and triggers extended marine oxygen holes. Proc. Natl. Acad. Sci. 106, 3017–3022. https://doi.org/10.1073/pnas.0813384106

Hovland, M., Judd, A.G., Burke, R.A., 1993. The global flux of methane from shallow submarine sediments. Chemosphere 26, 559–578. https://doi.org/10.1016/0045-6535(93)90442-8

Hylén, A., Taylor, D., Kononets, M., Lindegarth, M., Stedt, A., Bonaglia, S., Bergström, P., 2021. In situ characterization of benthic fluxes and denitrification efficiency in a newly re-established mussel farm. Sci. Total Environ. 782, 146853. https://doi.org/10.1016/j.scitotenv.2021.146853

Intergovernmental Panel On Climate Change, 2022. Climate Change and Land: IPCC Special Report on Climate Change, Desertification, Land Degradation, Sustainable Land Management, Food Security, and Greenhouse Gas Fluxes in Terrestrial Ecosystems, 1st ed. Cambridge University Press. https://doi.org/10.1017/9781009157988

Kotta, J., Futter, M., Kaasik, A., Liversage, K., Rätsep, M., Barboza, F.R., Bergström, L., Bergström, P., Bobsien, I., Díaz, E., Herkül, K., Jonsson, P.R., Korpinen, S., Kraufvelin, P., Krost, P., Lindahl, O., Lindegarth, M., Lyngsgaard, M.M., Mühl, M., Sandman, A.N., Orav-Kotta, H., Orlova, M., Skov, H., Rissanen, J., Šiaulys, A., Vidakovic, A., Virtanen, E., 2020. Cleaning up seas using blue growth initiatives: Mussel farming for eutrophication control in the Baltic Sea. Sci. Total Environ. 709, 136144. https://doi.org/10.1016/j.scitotenv.2019.136144

Kroeker, K.J., Kordas, R.L., Crim, R.N., Singh, G.G., 2010. Meta-analysis reveals negative yet variable effects of ocean acidification on marine organisms. Ecol. Lett. 13, 1419–1434. https://doi.org/10.1111/j.1461-0248.2010.01518.x

Lacroix, F., Ilyina, T., Mathis, M., Laruelle, G.G., Regnier, P., 2021. Historical increases in land-derived nutrient inputs may alleviate effects of a changing physical climate on the oceanic carbon cycle. Glob. Change Biol. 27, 5491–5513. https://doi.org/10.1111/gcb.15822

Lee, H.Z.L., Davies, I.M., Baxter, J.M., Diele, K., Sanderson, W.G., 2024. A blue carbon model for the European flat oyster (*OSTREA EDULIS*) and its application in environmental restoration. Aquat. Conserv. Mar. Freshw. Ecosyst. 34, e4030. https://doi.org/10.1002/aqc.4030

Lindahl, O., Hart, R., Hernroth, B., Kollberg, S., Loo, L.-O., Olrog, L., Rehnstam-Holm, A.-S., Svensson, J., Svensson, S., Syversen, U., 2005. Improving Marine Water Quality by Mussel Farming: A Profitable Solution for Swedish Society. Ambio 34, 131–138.

Little, D.C., Newton, R.W., Beveridge, M.C.M., 2016. Aquaculture: a rapidly growing and significant source of sustainable food? Status, transitions and potential. Proc. Nutr. Soc. 75, 274–286. https://doi.org/10.1017/S0029665116000665

Lyu, Z., Shao, N., Akinyemi, T., Whitman, W.B., 2018. Methanogenesis. Curr. Biol. CB 28, R727–R732. https://doi.org/10.1016/j.cub.2018.05.021

MacLeod, M., Gerber, P., Mottet, A., Tempio, G., Falcucci, A., Opio, C., Vellinga, T., Henderson, B., Steinfeld, H., 2013. Greenhouse gas emissions from pig and chicken supply chains – A global life cycle assessment.

Malyan, S.K., Bhatia, A., Kumar, A., Gupta, D.K., Singh, R., Kumar, S.S., Tomer, R., Kumar, O., Jain, N., 2016. Methane production, oxidation and mitigation: A mechanistic

understanding and comprehensive evaluation of influencing factors. Sci. Total Environ. 572, 874–896. https://doi.org/10.1016/j.scitotenv.2016.07.182

Mao, S.-H., Zhang, H.-H., Zhuang, G.-C., Li, X.-J., Liu, Q., Zhou, Z., Wang, W.-L., Li, C.-Y., Lu, K.-Y., Liu, X.-T., Montgomery, A., Joye, S.B., Zhang, Y.-Z., Yang, G.-P., 2022. Aerobic oxidation of methane significantly reduces global diffusive methane emissions from shallow marine waters. Nat. Commun. 13, 7309. https://doi.org/10.1038/s41467-022-35082-y

Marin, F., Luquet, G., Marie, B., Medakovic, D., 2007. Molluscan Shell Proteins: Primary Structure, Origin, and Evolution, in: Current Topics in Developmental Biology. Elsevier, pp. 209–276. https://doi.org/10.1016/S0070-2153(07)80006-8

McDougall, C., Degnan, B.M., 2018. The evolution of mollusc shells. WIREs Dev. Biol. 7, e313. https://doi.org/10.1002/wdev.313

Mejia, A., Harwatt, H., Jaceldo-Siegl, K., Sranacharoenpong, K., Soret, S., Sabaté, J., 2018. Greenhouse Gas Emissions Generated by Tofu Production: A Case Study. J. Hunger Environ. Nutr. 13, 131–142. https://doi.org/10.1080/19320248.2017.1315323

Murray, R.H., Erler, D.V., Eyre, B.D., 2015. Nitrous oxide fluxes in estuarine environments: response to global change. Glob. Change Biol. 21, 3219–3245. https://doi.org/10.1111/gcb.12923

Naylor, R.L., Kishore, A., Sumaila, U.R., Issifu, I., Hunter, B.P., Belton, B., Bush, S.R., Cao, L., Gelcich, S., Gephart, J.A., Golden, C.D., Jonell, M., Koehn, J.Z., Little, D.C., Thilsted, S.H., Tigchelaar, M., Crona, B., 2021. Blue food demand across geographic and temporal scales. Nat. Commun. 12, 5413. https://doi.org/10.1038/s41467-021-25516-4

Opio, C., Gerber, P., Mottet, A., Falucci, A., Tempio, G., MacLeod, M., Vellinga, T., Henderson, B., Steinfeld, H., 2013. Greenhouse gas emissions from ruminant supply chains – A global life cycle assessment.

Ray, N.E., Maguire, T.J., Al-Haj, A.N., Henning, M.C., Fulweiler, R.W., 2019. Low Greenhouse Gas Emissions from Oyster Aquaculture. Environ. Sci. Technol. 53, 9118–9127. https://doi.org/10.1021/acs.est.9b02965

Santos, I.R., Maher, D.T., Eyre, B.D., 2012. Coupling Automated Radon and Carbon Dioxide Measurements in Coastal Waters. Environ. Sci. Technol. 46, 7685–7691. https://doi.org/10.1021/es301961b

Scanfjord, Våra odlingar [WWW Document], 2024. URL https://www.scanfjord.se/vara-odlingar/ (accessed 5.7.24).

Shahidul Islam, Md., Tanaka, M., 2004. Impacts of pollution on coastal and marine ecosystems including coastal and marine fisheries and approach for management: a review and synthesis. Mar. Pollut. Bull. 48, 624–649. https://doi.org/10.1016/j.marpolbul.2003.12.004

Smith, K.A., 2005. The impact of agriculture and other land uses on emissions of methane and nitrous and nitric oxides. Environ. Sci. 2, 101–108. https://doi.org/10.1080/15693430500370423

Srinivasan, U.T., Cheung, W.W.L., Watson, R., Sumaila, U.R., 2010. Food security implications of global marine catch losses due to overfishing. J. Bioeconomics 12, 183–200. https://doi.org/10.1007/s10818-010-9090-9

Stief, P., Poulsen, M., Nielsen, L.P., Brix, H., Schramm, A., 2009. Nitrous oxide emission by aquatic macrofauna. Proc. Natl. Acad. Sci. 106, 4296–4300. https://doi.org/10.1073/pnas.0808228106

Suplicy, F.M., 2020. A review of the multiple benefits of mussel farming. Rev. Aquac. 12, 204–223. https://doi.org/10.1111/raq.12313

Tamburini, E., Turolla, E., Lanzoni, M., Moore, D., Castaldelli, G., 2022. Manila clam and Mediterranean mussel aquaculture is sustainable and a net carbon sink. Sci. Total Environ. 848, 157508. https://doi.org/10.1016/j.scitotenv.2022.157508

University of Gothenburg, Ships [WWW Document], 2023. URL https://www.gu.se/en/kristineberg/infrastructure-and-services/ships (accessed 4.10.24).

Voet, H., Soetaert, K., Moens, T., Bodé, S., Boeckx, P., Van Colen, C., Vanaverbeke, J., 2023. N2O production by mussels: Quantifying rates and pathways in current and future climate settings. Front. Mar. Sci. 10, 1101469. https://doi.org/10.3389/fmars.2023.1101469

Walter, S., Bange, H.W., Breitenbach, U., Wallace, D.W.R., 2006. Nitrous oxide in the North Atlantic Ocean. Biogeosciences 3, 607–619. https://doi.org/10.5194/bg-3-607-2006

Weiss, R.F., 1974. Carbon dioxide in water and seawater: the solubility of a non-ideal gas. Mar. Chem. 2, 203–215. https://doi.org/10.1016/0304-4203(74)90015-2

Weiss, R.F., Price, B.A., 1980. Nitrous oxide solubility in water and seawater. Mar. Chem. 8, 347–359. https://doi.org/10.1016/0304-4203(80)90024-9

Wood, J.D., 2017. Meat Composition and Nutritional Value, in: Lawrie´s Meat Science. Elsevier, pp. 635–659. https://doi.org/10.1016/B978-0-08-100694-8.00020-0

Yaghubi, E., Carboni, S., Snipe, R.M.J., Shaw, C.S., Fyfe, J.J., Smith, C.M., Kaur, G., Tan, S.-Y., Hamilton, D.L., 2021. Farmed Mussels: A Nutritive Protein Source, Rich in Omega-3 Fatty Acids, with a Low Environmental Footprint. Nutrients 13, 1124. https://doi.org/10.3390/nu13041124

Yamamoto, S., Alcauskas, J.B., Crozier, T.E., 1976. Solubility of methane in distilled water and seawater. J. Chem. Eng. Data 21, 78–80. https://doi.org/10.1021/je60068a029

Zhuang, M., Gongbuzeren, Li, W., 2017. Greenhouse gas emission of pastoralism is lower than combined extensive/intensive livestock husbandry: A case study on the Qinghai-Tibet Plateau of China. J. Clean. Prod. 147, 514–522. https://doi.org/10.1016/j.jclepro.2017.01.126